Pygo2 expands mammary progenitor cells by facilitating histone H3 K4 methylation

Bingnan Gu,[1] Peng Sun,[1] Yuanyang Yuan,[1,4,5] Ricardo C. Moraes,[6,7] Aihua Li,[1] Andy Teng,[1] Anshu Agrawal,[3] Catherine Rhéaume,[1] Virginia Bilanchone,[1] Jacqueline M. Veltmaat,[8] Ken-Ichi Takemaru,[9] Sarah Millar,[10,11] Eva Y.-H.P. Lee,[1] Michael T. Lewis,[6,7] Boan Li,[1,4,5] and Xing Dai[1,2]

[1]Department of Biological Chemistry, [2]Developmental Biology Center, and [3]Department of Medicine, University of California, Irvine, Irvine, CA 92697
[4]Department of Biomedical Sciences and [5]Key Laboratory of the Ministry of Education for Cell Biology and Tumor Cell Engineering, Xiamen University, Xiamen, Fujian 361005, People's Republic of China
[6]Lester and Sue Smith Breast Center and [7]Department of Molecular and Cellular Biology, Baylor College of Medicine, Houston, TX 77030
[8]Institute of Molecular and Cell Biology, A*STAR, Proteos, 138673 Singapore
[9]Department of Pharmacological Sciences, State University of New York, Stony Brook, Stony Brook, NY 11794
[10]Department of Dermatology and Department of [11]Cell and Developmental Biology, University of Pennsylvania School of Medicine, Philadelphia, PA 19104

Recent studies have unequivocally identified multipotent stem/progenitor cells in mammary glands, offering a tractable model system to unravel genetic and epigenetic regulation of epithelial stem/progenitor cell development and homeostasis. In this study, we show that Pygo2, a member of an evolutionarily conserved family of plant homeo domain–containing proteins, is expressed in embryonic and postnatal mammary progenitor cells. Pygo2 deficiency, which is achieved by complete or epithelia-specific gene ablation in mice, results in defective mammary morphogenesis and regeneration accompanied by severely compromised expansive self-renewal of epithelial progenitor cells. Pygo2 converges with Wnt/β-catenin signaling on progenitor cell regulation and cell cycle gene expression, and loss of epithelial Pygo2 completely rescues β-catenin–induced mammary outgrowth. We further describe a novel molecular function of Pygo2 that is required for mammary progenitor cell expansion, which is to facilitate K4 trimethylation of histone H3, both globally and at Wnt/β-catenin target loci, via direct binding to K4-methyl histone H3 and recruiting histone H3 K4 methyltransferase complexes.

Introduction

The importance of epigenetic regulation in development such as that of stem cells and in diseases such as cancer has been increasingly recognized (Sims et al., 2003; Niwa, 2007). Whether the chromatin adopts a condensed or open configuration is jointly governed by histone modification and DNA methylation, and this in turn controls gene expression. Histone methylation at lysine (K) residues has been associated with gene activation (e.g., K4 of histone H3) or repression (e.g., K9 and K27 of histone H3; Sims et al., 2003). Although much has been learned about chromatin control in embryonic and hematopoietic stem cells (Niwa, 2007; Cui et al., 2009), epigenetic mechanisms underlying the self-renewal and differentiation of tissue-specific epithelial stem/progenitor cells remain poorly understood.

The identification and characterization of multipotent mammary stem/progenitor cells (Shackleton et al., 2006; Stingl et al., 2006) make the mammary gland an excellent model to study both genetic and epigenetic control of epithelial stem cell development and homeostasis. Such study holds the potential to greatly enhance our understanding of how breast cancer cells arise. Recent evidence points to an important role for the epigenetic silencer Bmi1 in both mammary stem cells and their more committed progeny (Pietersen et al., 2008). To date, little is known about epigenetic activators that control the self-renewal and differentiation of mammary stem/progenitor cells.

The Pygopus (Pygo) family of proteins contains a highly conserved C-terminal plant homeo domain (PHD) often found in chromatin regulatory factors (Bienz, 2006). *Drosophila melanogaster Pygo*, which is a prototype of the family, was identified as a

B. Gu and P. Sun contributed equally to this paper.

Correspondence to Boan Li: bali@xmu.edu.cn; or Xing Dai: xdai@uci.edu

Abbreviations used in this paper: ChIP, chromatin immunoprecipitation; HMT, histone H3 K4 methyltransferase; MEC, mammary epithelial cell; MMTV, mouse mammary tumor virus; PHD, plant homeo domain; Pygo, Pygopus; SSKO, skin/mammary epithelia–specific knockout; TEB, terminal end bud; Wg, Wingless.

THE JOURNAL OF CELL BIOLOGY

highly specific downstream component of canonical Wingless (Wg; *Drosophila* Wnt) signaling (Belenkaya et al., 2002; Kramps et al., 2002; Parker et al., 2002; Thompson et al., 2002). Published data support two nonmutually exclusive models regarding the biochemical function of Pygo proteins: (1) they are recruited to β-catenin–lymphoid enhancer factor complex, which are nuclear effectors of Wg/Wnt signaling, via the adapter protein Legless/BCL9 and act as a transcriptional coactivator of the complex; (2) they facilitate nuclear retention of β-catenin (for review see Jessen et al., 2008). Of the two mammalian *Pygo* homologues, *Pygo2* is more broadly expressed and functionally important than *Pygo1* (Li et al., 2007; Schwab et al., 2007). *Pygo2* is required for the proper development of multiple tissues, whereas additional deletion of *Pygo1* does not appear to aggravate the *Pygo2* phenotype (Li et al., 2007; Schwab et al., 2007; Song et al., 2007; Nair et al., 2008). In contrast to *Drosophila Pygo*, *Pygo2* function in the two most extensively characterized *Pygo2*-requiring tissues, eye and testis, is independent of Wnt/β-catenin (Song et al., 2007; Nair et al., 2008; for review see Jessen et al., 2008). As such, genetic evidence for a functional interaction between mammalian *Pygo* genes and Wnt/β-catenin signaling is currently lacking.

In this work, we combine mouse genetics with biochemical approaches to study the function of Pygo2 in mammary stem/progenitor cells. We show that Pygo2 regulates mammary development by cell-intrinsically controlling the expansive self-renewal of epithelial progenitor cells. We provide evidence that Pygo2 regulates the expression of Wnt/β-catenin target genes, including those involved in cell cycle G1–S progression, and that loss of Pygo2 rescues β-catenin overexpression–induced mammary outgrowth. We present in vitro and in vivo data that Pygo2 facilitates the trimethylation of histone H3 K4 by binding to K4-methyl histone H3 and recruiting histone H3 K4 methyltransferase (HMT) complexes to bulk chromatin and Wnt target loci and that this chromatin function of Pygo2 is required for optimal expansive self-renewal of mammary progenitor cells.

Results

Pygo2 expression is enriched in developmental mammary stem/progenitor cells

To explore the function of Pygo2, we first examined its expression in embryonic and postnatal mammary glands using a polyclonal antibody against Pygo2 (Li et al., 2007). Mammary placode, representing a field of developmental mammary progenitor cells, forms between embryonic day (E) 10.5 and E11.5, and progresses through bud and sprout stages to give rise to a rudimentary mammary tree by birth (Fig. 1 A; Veltmaat et al., 2003). Nuclear Pygo2 protein was detected in placodal epithelium (not depicted) but became more prominent in actively growing mammary buds (Fig. 1 B). A few surrounding mammary mesenchymal cells also expressed Pygo2 (Fig. 1 B, arrowhead). After birth, the mammary gland enters a relatively quiescent stage but then expands rapidly via elongation and branching at around 3–7 wk of age, culminating in a mature gland by ∼10–12 wk (Fig. 1 C). Ductal morphogenesis is driven by the active proliferation of mammary progenitor cells that reside at the tip, or terminal end bud (TEB), of elongating

ducts, with TEB inner body and outer cap cells giving rise to luminal and basal/myoepithelial cells, respectively (Ball, 1998; Kenney et al., 2001; Woodward et al., 2005). Strong Pygo2 signals were observed in all body and some cap cells of the TEB in pubertal mammary glands (Fig. 1 D). As development proceeded and cells left the ductal tips, Pygo2 expression became downregulated (Fig. 1 E, arrow) such that in mature glands, nuclear Pygo2 was barely detectable (not depicted). During pregnancy, small structures bud off the ductal compartment and differentiate to form an expanded lobuloalveolar compartment composed of basal myoepithelium and secretory luminal epithelium (Fig. 1 F; Hennighausen and Robinson, 2001). Pygo2 expression became prominent again, particularly in the developing alveolar structures (Fig. 1 G). Together, these results demonstrate that Pygo2 is expressed in developmental mammary stem/progenitor cells, and its presence correlates with active proliferation of these cells.

Epithelial Pygo2 is required for mammary gland morphogenesis

To ask whether Pygo2 is required for mammary development, we first examined embryonic mammogenesis in *Pygo2*^{−/−} mice. Whole-mount skin preparations from *Pygo2*^{−/−} female embryos revealed mammary defects with a variable penetrance ranging from absence of any rudiment to impaired elongation and branching of the bud/sprout (Fig. 2, A and B). Most often, glands 1, 2, and 3 were visibly absent, and if present, never branched. Even in the least affected gland 4, branching morphogenesis was less advanced than in the wild type. The differential effect of *Pygo2* deletion is in keeping with the previous finding that different pairs of mammary glands respond differently to the same genetic mutations (Veltmaat et al., 2006).

To investigate the importance of epithelial Pygo2 in postnatal mammary development, we generated *Pygo2* skin/mammary epithelia–specific knockout (SSKO) mice by crossing a "floxed" *Pygo2* allele (Li et al., 2007) with transgenic mice expressing Cre under the K14 promoter (K14-Cre; Andl et al., 2004). The specificity and efficacy of K14-Cre was demonstrated by β-galactosidase expression in mammary placode and surrounding surface ectoderm (Fig. 2 C) as well as throughout the basal and luminal compartments of postnatal virgin mammary glands (Fig. 2 D and not depicted) of K14-Cre/Rosa26R mice. Rosa26R is a reporter line containing loxP-flanked lacZ that can be activated by Cre-mediated recombination (Zambrowicz et al., 1997). PCR of tissue genomic DNAs isolated from *Pygo2* SSKO (i.e., K14-Cre/*Pygo2*[flox/−]) mice confirmed skin epithelia–specific recombination at the *Pygo2* locus (Fig. 2 E). Although residual Pygo2-expressing cells were occasionally seen, a vast majority of mammary epithelial cells (MECs) in virgin SSKO females lacked detectable Pygo2 protein (Fig. 2 F).

Similar to *Pygo2*^{−/−} animals, mammary glands 1 and 2 in SSKO newborns were developmentally impaired (unpublished data). In contrast, gland 4 was indistinguishable from wild type at the newborn stage (unpublished data), allowing us to assess the role of Pygo2 in its postnatal development. The most remarkable defect was a lack of prominent TEB structures in 3-wk-old *Pygo2* SSKO females (Fig. 2 G, arrows). At 6 wk, ductal elongation was significantly delayed (Fig. 2 H), whereas by 9 wk, SSKO glands often contained fewer branches and lateral buds than control
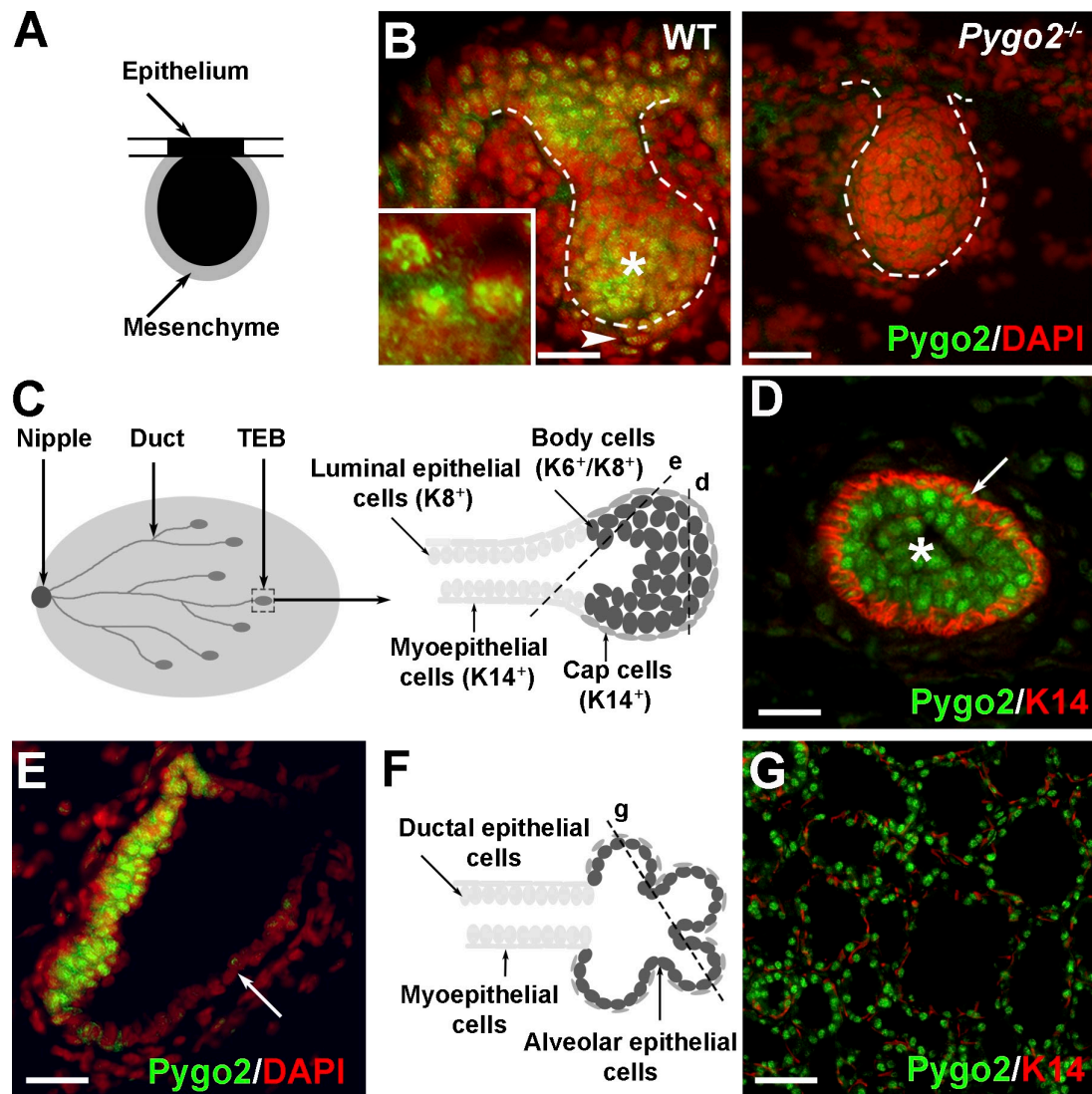
Figure 1. **Pygo2 expression in mammary epithelial progenitor cells.** (A, C, and F) Sketch diagrams showing anatomical features of embryonic (A), pubertal (C), and pregnant (F) mammary glands. (B, left) Strong Pygo2 expression in E15.5 mammary bud, particularly in the bulb region (asterisk). The inset is an enlarged image showing nuclear localization of Pygo2. The white dashed lines indicate basement membrane separating epithelial and mesenchymal compartments. The absence of signal in *Pygo2*^{−/−} mammary bud (right) confirms antibody specificity. The arrowhead points to Pygo2-expressing mesenchymal cells. (D) Pygo2 expression in cap (outlined by keratin 14[+] or K14[+]; arrow) and body cells (indicated by an asterisk) of TEBs from 3-wk-old females. (E) Pygo2 expression in 6-wk-old mammary epithelium. Note the reduced Pygo2 expression as cells leave the TEB (arrow). (G) Ubiquitous Pygo2 expression in lobuloalveolar cells of 18.5-d pregnant mammary glands. The planes of sections for D/E and G are indicated by the dashed lines in C and F, respectively. WT, wild type. Bars: (B) 30 µm; (D and E) 25 µm; (G) 50 µm.

glands (Fig. S1 A). Mammary defects persisted during pregnancy and lactation, as shown by apparently reduced alveolar formation and reduced milk production in some SSKO females (Fig. S1, B–D). In contrast, mammary gland morphology and function in *Pygo2*[flox/−] littermates were comparable with the wild type (Fig. S1 D and not depicted). Collectively, these results demonstrate that Pygo2 functions at least in part in the mammary epithelium to regulate critical aspects of mammogenesis, including elongation and branching of embryonic and postnatal mammary glands.

Pygo2 controls the expansion of mammary progenitor cells but is dispensable for their differentiation

To explore whether mammary stem cells are affected, we first performed FACS analysis of adult virgin control and SSKO

glands using known markers of multipotent mammary stem cells, namely Lin^{−}CD24^{+}CD29[High] (Shackleton et al., 2006). An approximately twofold reduction in Lin^{−}CD24^{+}CD29[High] cells was consistently observed in the mutant (Fig. 3 A). The Lin^{−}CD24^{+}CD29[High] population includes basally localized myoepithelial cells. Therefore, we examined the expression of K6, a marker of multi/bipotent early progenitor cells that are likely immediate progeny of the stem cells (Smith et al., 1990; Grimm et al., 2006; Stingl et al., 2006). At the ages (3–9 wk after birth) when K6 expression was readily observed in control glands, there was a significant reduction to near absence of K6^{+} cells in mutant TEBs and ducts (Fig. 3 B). A reduced presence of K6^{+} cells was also evident in Pygo2-deficient embryonic mammary gland, but this reduction was less remarkable than in the adult (Fig. S2 A). The progressive loss of K6[+] progenitor
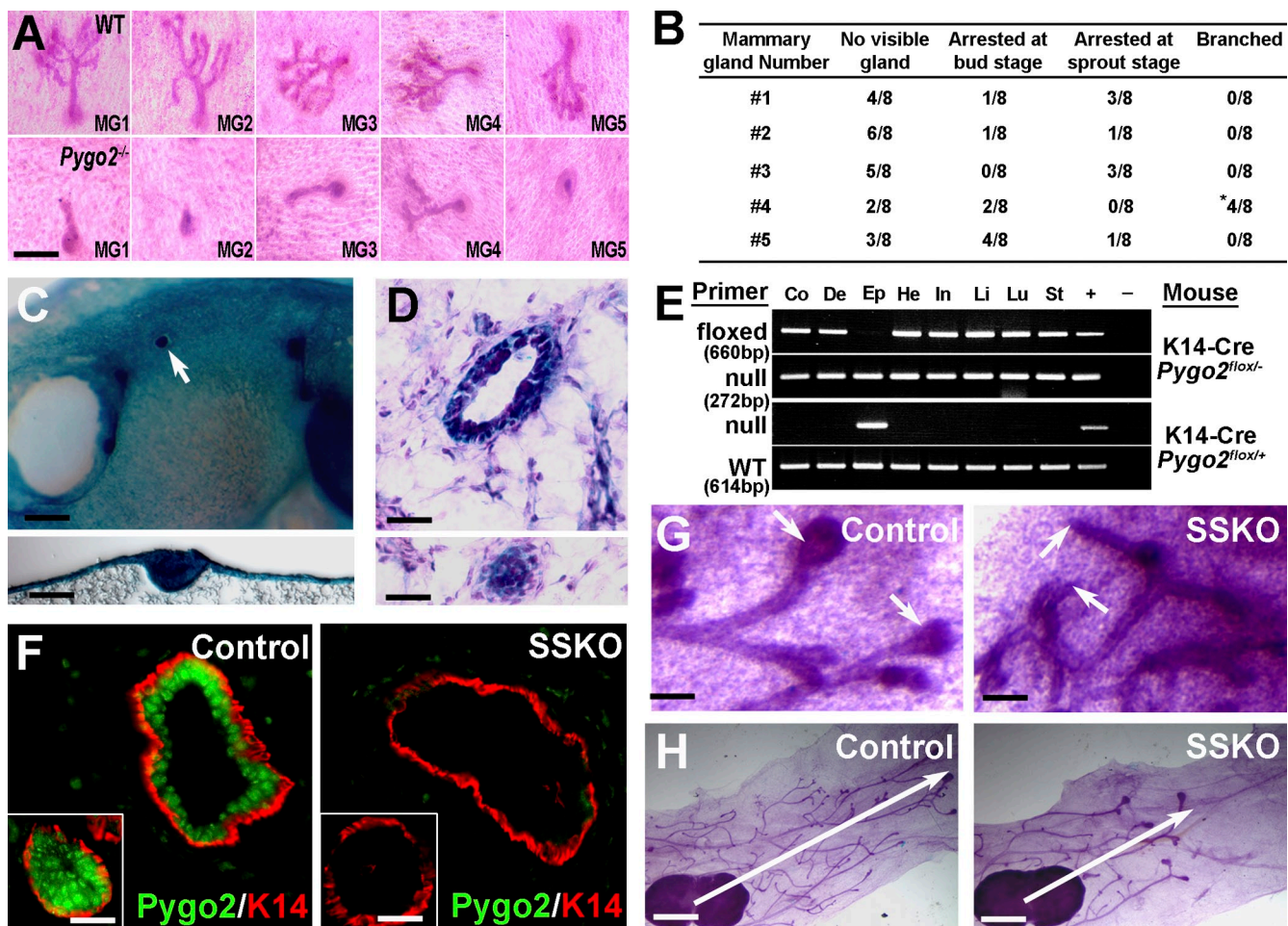
Figure 2. Embryonic and postnatal mammary phenotypes of Pygo2-deficient mice. (A) Whole-mount preparations of carmine-stained skins of E18.5 wild-type (WT; top) and *Pygo2^−/−^* (bottom) embryos showing select individual mammary glands (MG). (B) Summary of results obtained on all ten glands from multiple mutant embryos ($n = 4$). The mean branching point is calculated to be $3.25 ± 0.63$ and $6.5 ± 1.04$ for mutant and wild type, respectively (asterisk; $P = 0.04$). (C) Whole-mount LacZ-stained skin preparation of an E11.5 K14-Cre/Rosa26R embryo. A transversal section of placode 3 (arrow) is shown at the bottom. (D) LacZ-stained cross sections (counterstained with hematoxylin and eosin) through mammary duct (top) and TEB (bottom) of a 3-wk-old K14-Cre/Rosa26R female. (E) Genomic PCR of *Pygo2* alleles showing recombination in epidermis but not dermis or other tissues. Co, colon; De, dermis; Ep, epidermis; He, heart; In, intestine; Li, liver; Lu, lung; St, stomach. The plus and minus signs denote the controls for PCR. (F) Absence of Pygo2 in ductal epithelia and TEBs (insets) of virgin SSKO mammary glands. (G and H) Carmine red–stained whole-mount preparations of mammary gland 4 from 3-wk-old ($n = 4$; G) and 6-wk-old ($n = 3$; H) females. Note the absence of TEB structures (short arrows in G) and the defective ductal elongation (marked by long arrows in H) in mutants. The control genotypes shown are K14-Cre/*Pygo2^flox/+^* (F and G) and *Pygo2^flox/+^* (G). Bars: (A) 112 µm; (C) 30 µm; (D and F) 25 µm; (G) 107 µm; (H) 937 µm.

cells is consistent with an expansion defect. In contrast, no reduction was seen for ER$^+$/PR$^+$ hormone-sensing cells (Fig. 3 C and Fig. S2 B; Sleeman et al., 2007). Moreover, the expression of GATA-3 and TCF4, two transcription factors normally expressed in luminal epithelial cells (Barker et al., 1999; Kouros-Mehr et al., 2006; Asselin-Labat et al., 2007), and of NKCC1, a ductal luminal epithelial marker (Moore-Hoon and Turner, 1998; Miyoshi et al., 2001), was comparable between control and SSKO mammary glands (Fig. S2, C–E). Finally, gene expression analysis revealed increased mRNA levels of luminal keratin and alveolar differentiation markers, including K8, K18, K19, and κ-casein (Fig. S2, F and G), likely reflecting an imbalance in the numbers of mature luminal cells versus stem/progenitor cells.

To investigate the effect of Pygo2 deficiency on mammary stem/progenitor cell activity, we performed limiting dilution transplantations using primary MECs isolated from SSKO and control mice. Under the dilutions tested, Pygo2-deficient cells showed a nonstatistically significant decrease in the rate of successful transplantation (take rate) but displayed significantly less extensive mammary outgrowth (percent of fat pad filled) when compared with contralaterally injected wild-type cells (Fig. 3 D). We also seeded MECs at clonal densities on Matrigel to determine their differentiation potential in vitro. Control cells produced many colonies: some were large and composed of solid and lumen-containing structures reminiscent of those formed by isolated multipotent stem and/or early progenitor cells (Stingl et al., 2006), whereas others were small, with a distinct acinar morphology reminiscent of those formed by more differentiated progenitor cells (Fig. 3 E and not depicted). In SSKO mutant culture, the number of large, solid colonies was reduced (unpublished data). Importantly, many control colonies contained K6$^+$ cells, whereas the number of both K6$^+$ colonies and K6$^+$ cells per positive colony were greatly reduced in the
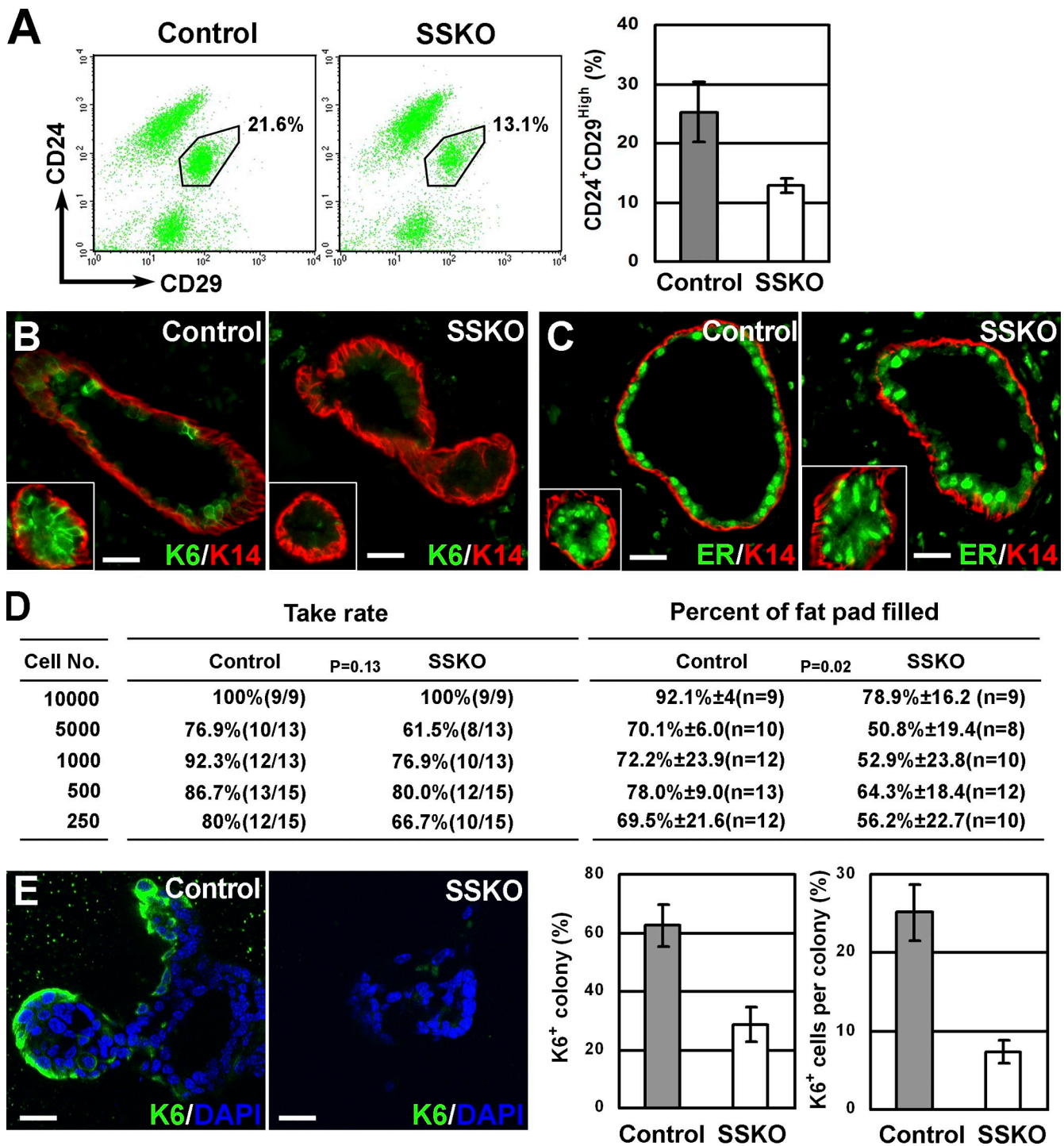
Figure 3. ***Pygo2* SSKO mammary epithelium contains fewer stem/progenitor cells.** (A) Results of FACS analysis revealing a decreased number of Lin⁻CD24⁺CD29^{High} cells in 10-wk-old Pygo2-deficient mammary glands. Representative FACS profiles from a single pair are shown on the left, and mean values from three different pairs are shown on the right. (B) Reduced presence of K6⁺ progenitor cells in 8-wk-old Pygo2-deficient mammary duct and ductal termini (insets). (C) ER expression is not affected by Pygo2 loss. (D) Representative results from limiting dilution transplantations of MECs derived from 9–12-wk-old control or *Pygo2* SSKO (*n* = 6) mice. (E) Reduced colony formation and K6 expression in Matrigel culture of MECs isolated from 8-wk-old SSKO mice. A quantitative analysis (right) reveals a statistically significant reduction in the number of K6⁺ colonies and K6⁺ cells per positive colony. The control genotypes shown are two *Pygo2^{flox/+}* and one wild type (A), *Pygo2^{flox/+}* (B), K14-Cre/*Pygo2^{flox/+}* (C), four *Pygo2^{flox/+}* and two K14-Cre/*Pygo2^{flox/+}* (D), and two K14-Cre/*Pygo2^{flox/+}* and one *Pygo2^{flox/+}* (E). (A and E) Error bars represent standard deviation. Bars: (B and C) 25 µm; (E) 37.5 µm.

mutant (Fig. 3 E). Collectively, our results demonstrate that *Pygo2* deletion adversely affects the expansion of mammary stem/progenitor cells while leaving the biochemistry and differentiation of mammary epithelium largely intact.

Pygo2 regulates MEC cell cycle progression

Active proliferation drives the expansive self-renewal of stem/progenitor cells during development. Therefore, we compared the proliferative activity of developmental progenitor cells in
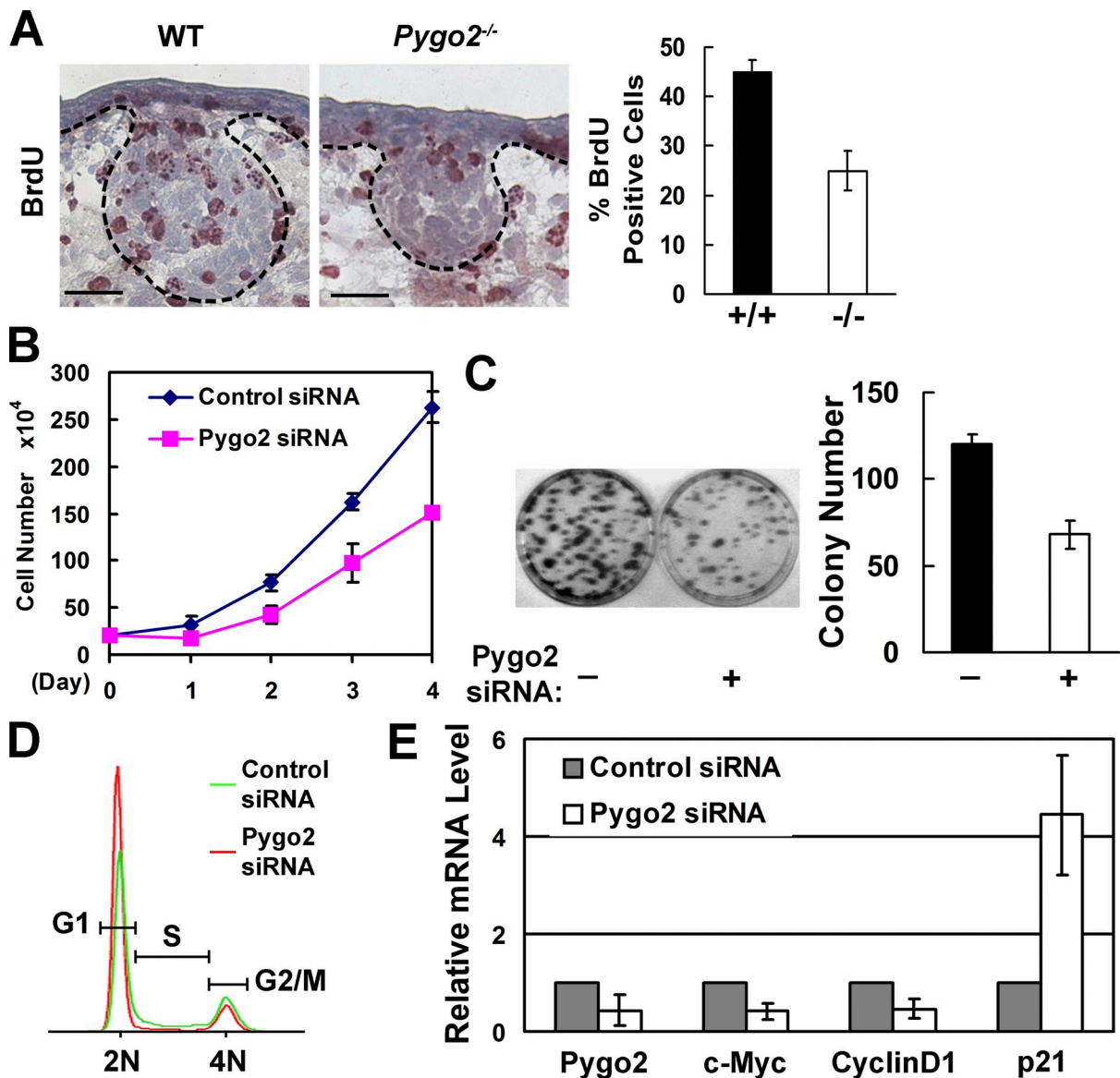
Figure 4. **Loss of Pygo2 leads to reduced mammary epithelial proliferation and compromised G1–S transition.** (A) Immunohistochemical detection of BrdU incorporation in mammary buds of E15.5 control and *Pygo2⁻/⁻* embryos. The BrdU-labeling index, calculated as the percent of BrdU-positive cells per total number of cells in mammary buds, is shown on the right. $P < 0.001$. The dashed lines indicate the basement membranes. WT, wild type. (B) Reduced growth of Pygo2-depleted MCF10A cells in high-density culture. (C) Reduced colony formation by Pygo2-depleted cells. (D) Cell cycle analysis of control and Pygo2-depleted cells. (E) Altered expression of cell cycle genes in Pygo2-depleted cells. mRNAs were collected 3 d after siRNA transfection and quantified by quantitative RT-PCR. (A–C and E) Error bars represent standard deviation. Bars, 20 μm.

normal and *Pygo2⁻/⁻* mammary buds. Buds from *Pygo2⁻/⁻* embryos contained fewer BrdU-incorporating cells than their wild-type counterparts (Fig. 4 A), indicating that Pygo2-deficient progenitor cells are less proliferative. There was no significant change in the number of apoptotic cells, as visualized by TUNEL staining (unpublished data). We also analyzed pregnant females and observed a reduction in alveologenesis-associated proliferation in a subset of Pygo2-deficient mammary glands (Fig. S1 E). Based on these findings, we surmise that Pygo2 regulates the proliferation but not survival of mammary epithelial progenitor cells.

In vitro passaging of MECs derived from *Pygo2* SSKO mice resulted in a culture population composed mostly of Pygo2-positive cells (Fig. S3 A), suggesting that residual Pygo2 expression confers a selective growth advantage. To analyze cell cycle progression directly, we turned to siRNA knockdown to acutely deplete Pygo2 in MCF10A cells, an immortal, nontransformed human MEC line which possess mammary progenitor cell activity (Fig. S3 B) and which expresses progenitor-associated genes (Neve et al., 2006). Efficient knockdown of Pygo2 was achieved and could be maintained in culture for >96 h (unpublished data). When cells were cultured at a high density, a significant decrease in growth rate was observed when Pygo2 was depleted (Fig. 4 B). When plated at a clonal density, a significant decrease in the number and size of colonies was observed for Pygo2-depleted cells (Fig. 4 C). FACS analysis of DNA content revealed a larger G1 population and a smaller S/G2/M population in Pygo2-depleted high-density culture than control (Fig. 4 D). These findings suggest that Pygo2 cell-intrinsically regulates
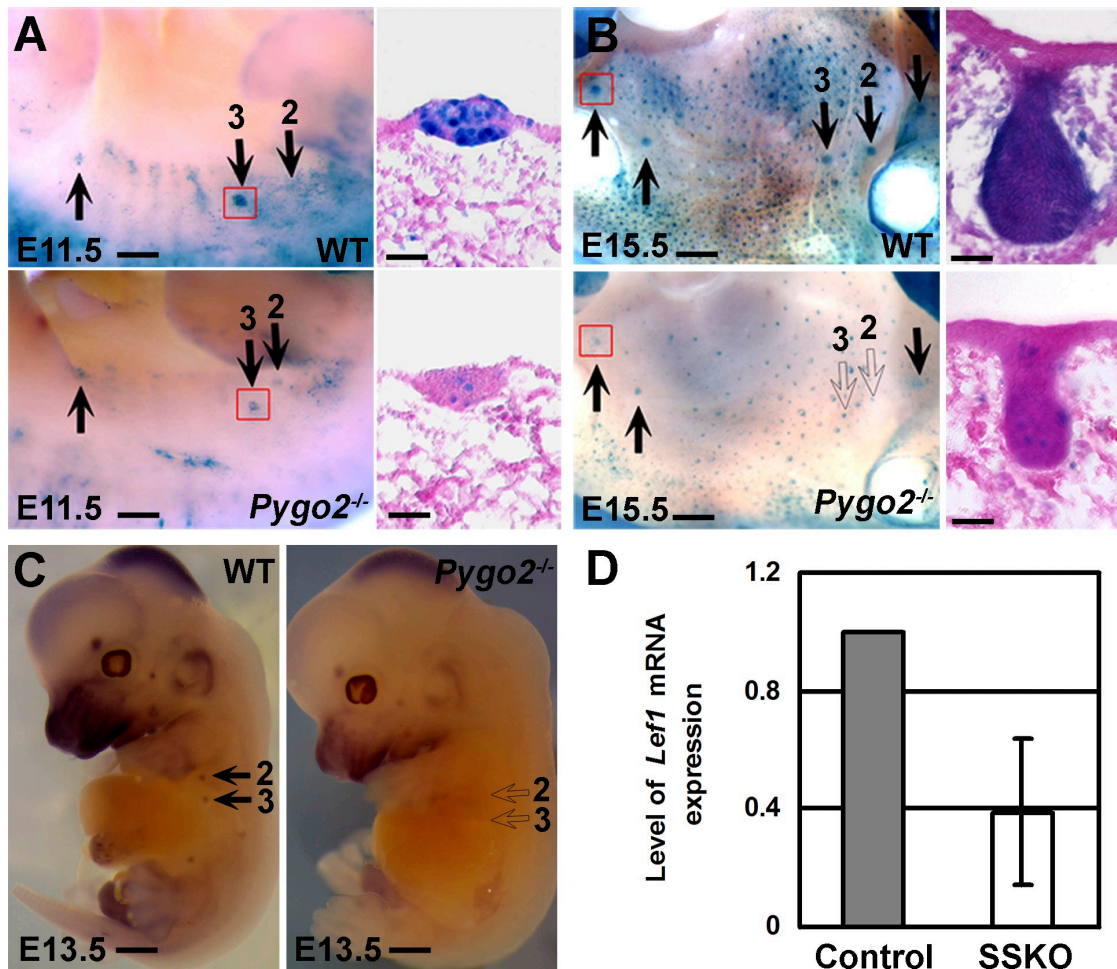
Figure 5. **Pygo2 is required for Wnt/β-catenin target gene expression in mammary epithelium.** (A and B) Whole-mount LacZ staining of *Pygo2* wild-type (WT; top) and deficient (bottom) BAT-gal embryos at E11.5 (A) and E15.5 (B). Numbers (2 and 3) next to the arrows indicate mammary buds 2 and 3. Corresponding sections of the boxed areas are shown on the right. Closed and open arrows indicate externally visible and invisible mammary glands, respectively. (C) Whole-mount in situ hybridization for *Lef1* on E13.5 wild-type and mutant embryos. (D) Results of quantitative RT-PCR showing reduced *Lef1* expression in *Pygo2* SSKO mammary glands (n = 3). The error bar represents standard deviation. Bars: (A) 195 μm; (B) 315 μm; (C) 900 μm; (insets) 20 μm.

mammary progenitor cell proliferation by promoting cell cycle G1–S progression. Consistent with this function, we observed reduced mRNA expression of c-Myc and cyclin D1, which normally promotes G1–S transition, and increased expression of p21$^{WAF1/cip1}$ (referred to as p21 from here on), which is an inhibitor of cyclin-dependent kinase required for G1–S transition, in Pygo2-depleted cells (Fig. 4 E).

Decreased Wnt/β-catenin target gene expression and rescue of β-catenin overexpression–induced mammary outgrowth in Pygo2-deficient animals

The mammary stem/progenitor cell phenotype of Pygo2-deficient mice mirrors that in Wnt-activating mutants (Li et al., 2003; Shackleton et al., 2006), raising the possibility that Pygo2 is involved in Wnt/β-catenin signaling in mammary epithelium. To address this, we first generated *Pygo2*$^{-/-}$ animals carrying a transgenic BAT-gal Wnt reporter gene that expresses β-galactosidase at sites where canonical Wnt signaling is active (Maretto et al., 2003). Strong β-galactosidase expression was seen persistently in

mammary rudiments of E11.5 to E15.5 *Pygo2*$^{+/+}$/BAT-gal embryos, whereas expression was significantly reduced in *Pygo2*$^{-/-}$/BAT-gal littermates (Fig. 5, A and B; and not depicted). The extent of reduction was greatest in mammary buds 2 and 3, correlating with their most severe morphological defects. We also examined the expression of *Lef1*, an endogenous Wnt/β-catenin target (Hovanes et al., 2001; Filali et al., 2002). Normally, *Lef1* is expressed in the developing mammary epithelium (Mailleux et al., 2002); however, in *Pygo2*$^{-/-}$ mammary buds, its mRNAs were barely detectable (Fig. 5 C). In contrast, the expression of another early mammary epithelial marker, *Wnt10b* (Veltmaat et al., 2004), was unaffected (Fig. S4). Reduced *Lef1* mRNA expression was also seen in postnatal mammary glands of *Pygo2* SSKO mice (Fig. 5 D). Collectively, these results demonstrate that Pygo2 is required in vivo for gene expression downstream of Wnt/β-catenin signaling.

To test the genetic interaction between Pygo2 and Wnt/β-catenin signaling, we first examined postnatal mammary morphogenesis in two mouse models in which Wnt/β-catenin signaling is aberrantly activated. K14-ΔN–β-catenin transgenic
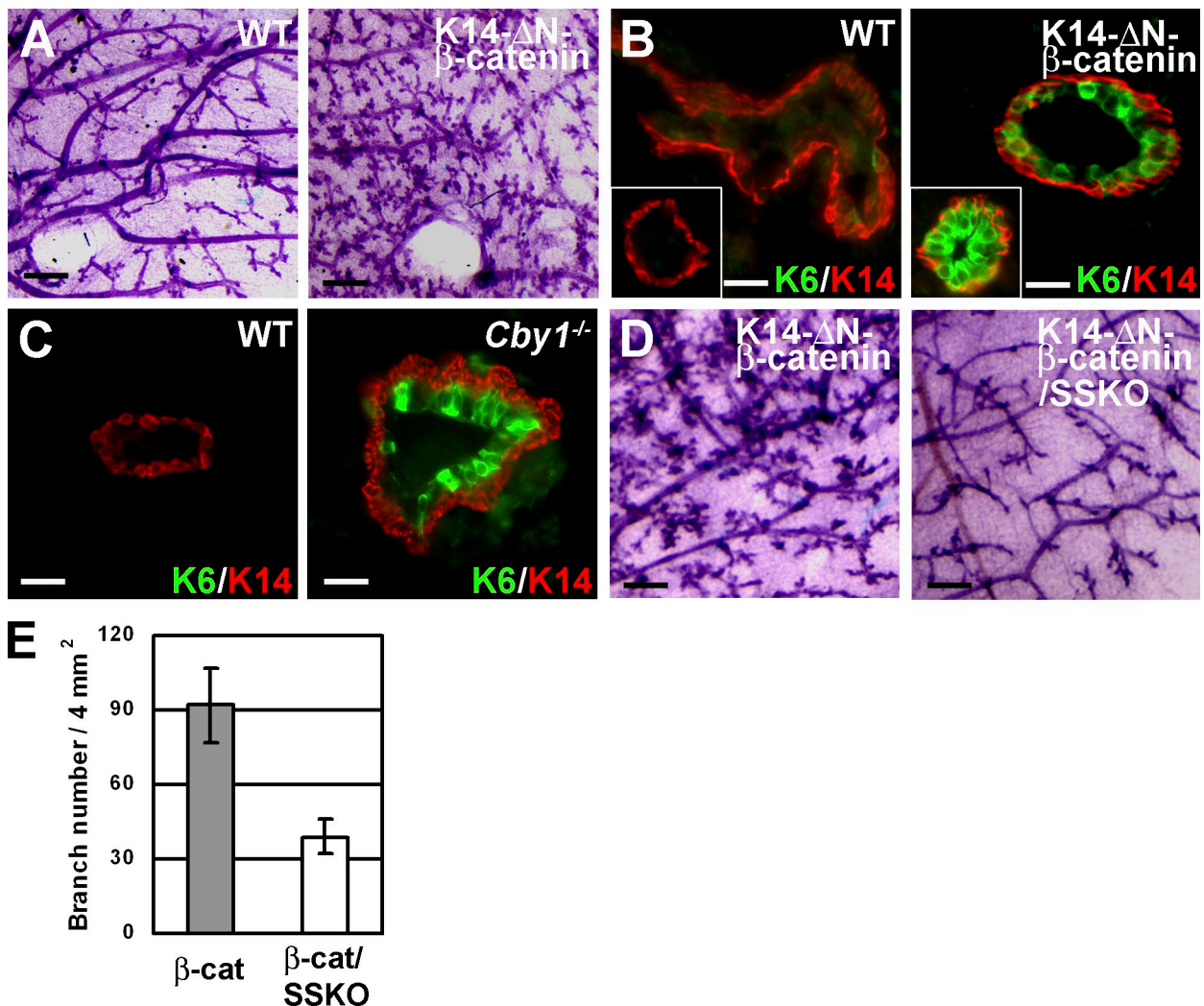
Figure 6. Loss of Pygo2 rescues the mammary outgrowth phenotype of K14-ΔN–β-catenin mice. (A) Whole-mount carmine staining of mammary glands from 12-wk-old wild-type (WT) and K14-ΔN–β-catenin (*n* = 5) females. (B and C) Persistent K6 expression in adult glands from K14-ΔN–β-catenin (12 wk old; B, right) and *Cby1*$^{-/-}$ (39 wk old; C, right) mice. The basal compartment is outlined by K14 staining. The insets show images of TEBs. (D) Whole-mount carmine-stained skin of 12-wk-old K14-ΔN–β-catenin and K14-ΔN–β-catenin/*Pygo2* SSKO (*n* = 4) littermates. (E) Quantitative analysis of branch points. Error bars represent standard deviation. β-cat, β-catenin. Bars: (A and D) 500 μm; (B and C) 25 μm.

mice express a stabilized form of β-catenin under the K14 promoter (Gat et al., 1998). Compared with wild-type littermates, transgenic virgin females showed precocious branching and lateral bud formation (Fig. 6 A). Moreover, at an age (>12 wk) when wild-type glands no longer contained an appreciable number of K6$^+$ cells, K14-ΔN–β-catenin transgenic mammary glands often displayed a persistent existence of such cells (Fig. 6 B). Prolonged accumulation of K6$^+$ cells was also observed when *Cby1*, a negative regulator of nuclear β-catenin (Takemaru et al., 2003; Voronina et al., 2009), was deleted (Fig. 6 C). We note that these phenotypes are not fully penetrant; instead, there is an inverse correlation between increased K6$^+$ cells and morphological overgrowth (unpublished data), implying that K6$^+$ cells are a transient population. To examine whether loss of Pygo2 rescues K14-ΔN–β-catenin–induced mammary overgrowth, we generated K14-Cre/*Pygo2*$^{flox/-}$/K14-ΔN–β-catenin females. Mammary glands from these mice were indistinguishable from control littermates and no longer showed precocious outgrowth

(Fig. 6, D and E). These findings provide in vivo evidence that Pygo2 interacts with Wnt/β-catenin signaling to regulate mammary epithelial morphogenesis.

Pygo2 binds to K4 di- and trimethylated histone H3, and this binding is important for mammary progenitor cell proliferation

Pygo2 contains a PHD, which has recently emerged as a recognition motif of K4 trimethylated histone H3 (H3K4me3; Pena et al., 2006; Shi et al., 2006; Taverna et al., 2006; Wysocka et al., 2006). Sequence alignment revealed that Pygo2 PHD contains several amino acids (for example, tryptophan [W] 352) that are present at similar positions in PHD of the H3K4me3-binding ING2 (Fig. 7 A). We generated and purified bacterially expressed Pygo2 PHD fused to GST (GST–Pygo2 PHD) and performed pull-down assays to examine its binding to native histones purified from calf thymus. Specific binding of GST–Pygo2 PHD but not GST to histones was observed (Fig. 7 B),

and Western blotting confirmed the enriched presence of H3K4me3 in GST–Pygo2 PHD pull-down samples (Fig. 7 C). In coimmunoprecipitation experiments, anti-Pygo2 antibody but not control IgG immunoprecipitated H3K4me3 from nuclease-digested chromatin prepared from cultured cells (Fig. 7 D). The ability of Pygo2 PHD to bind to biotinylated histone H3 N-terminal peptides was also tested. Binding was observed for K4 di- and trimethylated peptides, but not for unmethylated or K4 monomethylated peptides (Fig. 7 E). Importantly, the W352 to A mutation completely abolished Pygo2 binding to H3K4me2/3 peptides. In summary, these experiments uncover a new molecular function of Pygo2, which is binding to H3K4me2 and H3K4me3, two histone marks associated with active chromatin.

To delineate further H3K4me2/3-interacting residues in Pygo2 PHD, we generated and purified recombinant GST–Pygo2 PHD fusion proteins containing additional mutations at conserved residues and tested them using the native histone-binding assay. We also tested the ability of these proteins to bind to a 6× His–tagged HD1 domain of adapter protein BCL9 (Townsley et al., 2004). Three classes of mutations were identified: (1) those affecting both H3K4me2/3 and BCL9 binding (W352, M360, and T361), (2) those affecting only H3K4me2/3 binding (Y327), and (3) those affecting primarily BCL9 binding (A364 and L368; Fig. 7 F). Next, we repeated the binding assay but this time including a third component. An enhancement in PHD–BCL9 (HD1) interaction was observed when histones were added (Fig. 7 G, top; compare lanes 6 and 7 with lane 2). Moreover, BCL9 HD1 was able to interact with H3K3me3 when Pygo2 PHD was present (Fig. 7 G, bottom; compare lane 7 with lane 5). These results suggest that Pygo2–H3K4me3 and Pygo2–BCL9 (thus β-catenin) interactions are not mutually exclusive but instead are synergistic.

Next, we performed colony formation assay to assess the functional importance of Pygo2–H3K4me2/3 interaction. The introduction of exogenous full-length Pygo2 to MCF10A cells enhanced their colony formation (Fig. 7 H). The Y327A mutation abolished this enhanced colony-forming capacity, whereas the L368A mutation had a less detrimental effect. A deletion of the PHD led to colony formation at a level even below that achieved with vector control, suggesting a dominant-negative effect. Therefore, Pygo2 binding to both H3K4me2/3 and BCL9/β-catenin is important for its function in mammary progenitor cell expansion, with binding to H3K4me2/3 contributing more significantly than its previously known interaction with BCL9/β-catenin (Townsley et al., 2004).

Pygo2 facilitates H3 K4 trimethylation by recruiting WDR5, a core component of histone HMT complexes, to target chromatin

Next, we asked whether Pygo2 regulates H3 K4 methylation in MECs. A significant reduction in the level of extractable H3K4me3 was observed when Pygo2 was depleted from MCF10A cells (Fig. 8 A). At high concentrations of Pygo2 siRNA, the level of total histone H3 was also reduced; however, the decrease in H3K4me3 was quantitatively more remarkable.
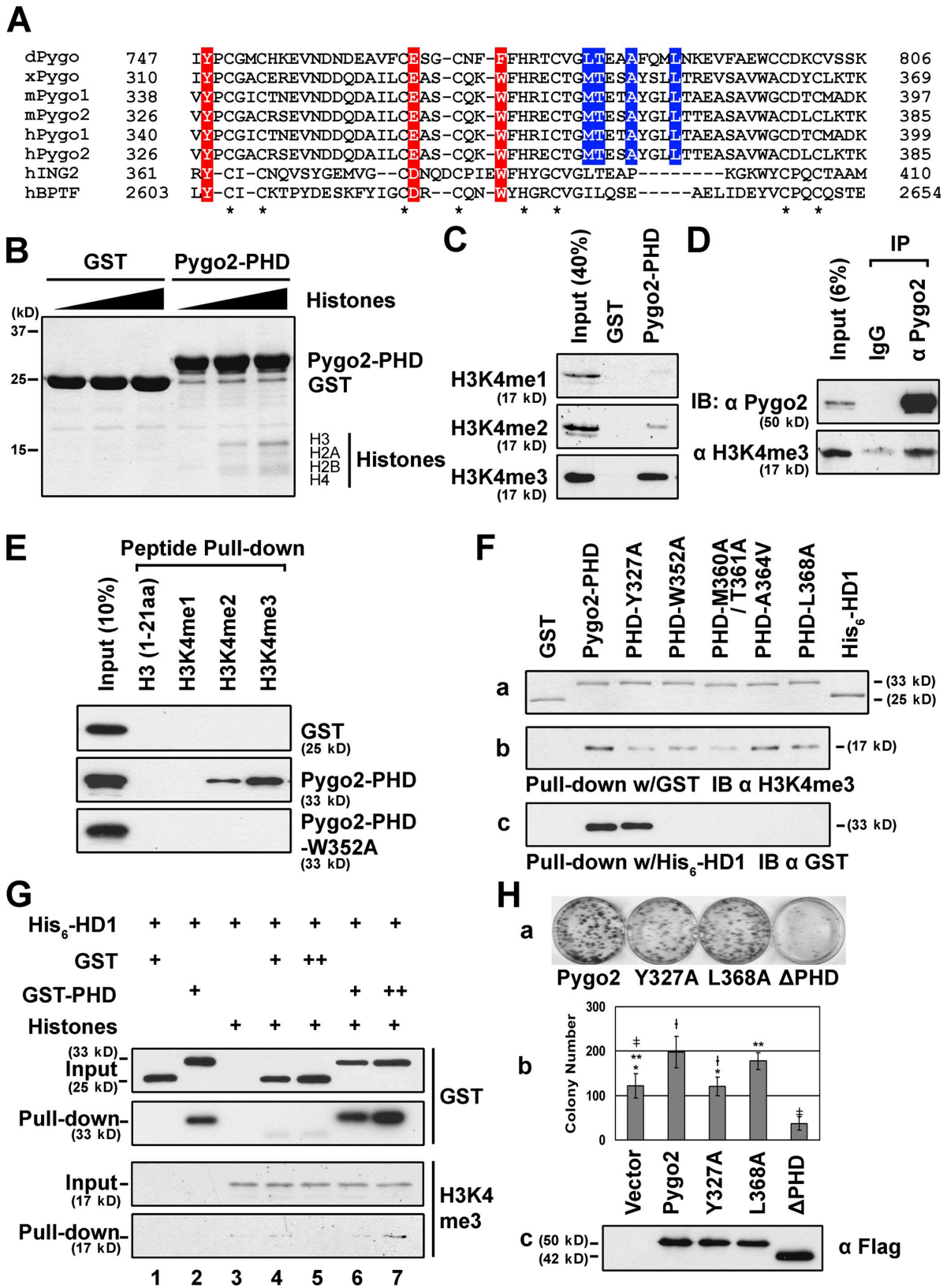
A reduction in H3K4me2 level also occurred, whereas the levels of H3K4me1, H3K9me3, and H3K27me3 were not significantly affected (Fig. 8 B). Supporting these cell culture experiments, we detected a dramatically reduced level of H3K4me3 in *Pygo2* SSKO mammary glands (Fig. 8 C). To examine whether reduced H3K4me3 occurs at specific Wnt/β-catenin target loci, we performed chromatin immunoprecipitation (ChIP) analysis on c-Myc enhancer (He et al., 1998; van de Wetering et al., 2002) and *Lef1* promoter (Hovanes et al., 2001) using primers that amplify regions encompassing lymphoid enhancer factor/T cell factor–binding sites. In both cases, we observed high levels of H3K4me3 at these Wnt/β-catenin–responsive genomic regions and a statistically significant reduction when Pygo2 was depleted (Fig. 8 D).

The specific effect of Pygo2 depletion on H3K4me2/3 is reminiscent of that seen when core components of SET domain HMT complexes are depleted (Wysocka et al., 2005; Dou et al., 2006). Therefore, we asked whether Pygo2 physically associates with WDR5, an essential and common component of SET domain HMT complexes (Wysocka et al., 2005). Anti-Pygo2 antibody immunoprecipitated WDR5 from 293T cells both in the absence and presence of BIO, an inhibitor of intracellular GSK3β which increases nuclear β-catenin levels (Fig. 8 E; Sato et al., 2004). In contrast, Pygo2 interaction with β-catenin was evident only when BIO was present. Pygo2–WDR5 interaction was also observed in MCF10A cells stably transfected with a Flag-tagged Pygo2 protein (Fig. 8 F). Together, these experiments demonstrate that Pygo2 physically associates with WDR5 and that this interaction is likely independent of nuclear β-catenin.

To test whether Pygo2 facilitates chromatin association of WDR5, we prepared bulk chromatin (Mendez and Stillman, 2000) from MCF10A cells transfected with Pygo2 or control siRNA. Although WDR5 readily associated with the chromatin in control cells, little association was detected when Pygo2 was depleted (Fig. 8 G). In ChIP experiments, we detected specific binding of WDR5 to Wnt/β-catenin–responsive regions in the c-Myc enhancer and *Lef1* promoter and saw that this binding was dramatically reduced when Pygo2 was depleted (Fig. 8 H). Similar findings were made on the cyclin D1 promoter, which is another direct target of Wnt/β-catenin (Tetsu and McCormick, 1999; unpublished data). Therefore, Pygo2 is required for efficient association of WDR5 with bulk chromatin as well as at Pygo2/Wnt/β-catenin target loci in mammary progenitor cells.

Discussion

In this work, we describe, for the first time, important biological and mechanistic functions of chromatin regulator Pygo2 in mammary gland development and regeneration. Although the *Drosophila* studies discussed in the Introduction section have previously elucidated a genetic connection between *Drosophila* Pygo and Wg signaling, our work provides the first in vivo evidence that Pygo2 functionally participates in Wnt/β-catenin signaling in a mammalian tissue. Although we use mammary cells as a model system, these findings are likely applicable to other epithelial tissues that require Pygo2 and Wnt/β-catenin signaling for their development and regeneration.

Figure 7. **The H3K4me2/3-binding activity of Pygo2 is required for colony formation by mammary progenitor cells.** (A) Sequence alignment of PHD fingers in Pygo and ING2/bromodomain PHD finger transcription factor (BPTF) proteins. Note that the residues critical for H3K4me3 binding in ING2 and bromodomain PHD finger transcription factor (highlighted in red) are conserved among Pygo PHDs. Residues required for BCL9 binding are highlighted in blue. The asterisks represent conserved cysteine and histidine amino acids of the C_4HC_3 PHD. (B) Coomassie blue staining of calf thymus histone pull-downs. (C) Western blot analysis of pull-down samples in B with antibodies against mono-, di-, and trimethylated H3 K4. (D) Coimmunoprecipitation/Western blot analysis of Pygo2–H3K4me3 interaction in 293T cells. (E) Pull-down of histone H3 N-terminal peptides, with eluates analyzed by Western blotting with

Pygo2, mammary progenitor cell expansion, and cell cycle control

Early embryonic mammary progenitor cells switch from a dormant to an actively expanding state during the bud to sprout transformation (Veltmaat et al., 2003). Although stem cells in a homeostatic adult tissue are presumably quiescent (Chepko and Smith, 1997; Woodward et al., 2005), expansive self-renewal of mammary stem/progenitor cells is essential during postnatal development and for regeneration to occur after transplantation (Smith, 2005). Our study identifies Pygo2 as a novel biomarker of expanding mammary progenitor cells. More importantly, our parallel analysis of conventional and tissue-specific *Pygo2*-null mutant mice demonstrates that both embryonic progenitor cell proliferation and postnatal progenitor cell expansion require Pygo2. Thus, at least some common regulatory circuits are shared by embryonic and postnatal mammary progenitor cells. That said, mammary morphogenesis and regeneration are crippled but not abolished in the absence of Pygo2, leaving open the possibility of functional redundancy from Pygo1.

How does Pygo2 facilitate progenitor cell expansion? Molecular mechanisms, including the use of cell cycle inhibitors such as p21, exist to prevent quiescent stem cells from entering active cell cycle in bone marrow, skin, and forebrain (Topley et al., 1999; Cheng et al., 2000; Kippin et al., 2005). Indeed, p21 expression is enriched in a subset of label-retaining mammary cells (Clarke, 2005; Clarke et al., 2005). Conceivably, for expansive self-renewal to occur, stem/progenitor cells must possess the ability to counteract cell cycle inhibition. We found that loss of Pygo2 leads to a G1 stall of the cell cycle, accompanied by decreased c-Myc and cyclin D1 expression as well as increased p21 expression. These results suggest that Pygo2 empowers mammary stem/progenitor cells with the capacity to expand by directly or indirectly regulating critical cell cycle genes, thereby promoting G1–S transition.

Pygo2 and Wnt signaling in mammary epithelium

We have extensively probed into the involvement of mammary epithelial Pygo2 in Wnt signaling using both mouse models and molecular analyses. First, we uncover a mammary phenotype in Pygo2-deficient mice that is consistent with loss of Wnt/β-catenin signaling. The differential impairment of *Pygo2*$^{-/-}$ mammary rudiments is reminiscent of mammary placodes 2 and 3 suffering most severely from a homozygous *Lef1*-null mutation (van Genderen et al., 1994; Boras-Granic et al., 2006; unpublished data). The morphological defects of *Pygo2* SSKO mice are similar to those of mice deficient for Lrp5, a Wnt coreceptor (Lindvall et al., 2006). *Pygo2* SSKO mice have a decreased,

whereas mouse mammary tumor virus (MMTV)–Wnt1 mice have an increased number of Lin$^-$CD24$^+$CD29^{High} cells in their mammary glands (Shackleton et al., 2006). Moreover, loss of Pygo2 leads to a decreased K6$^+$ mammary progenitor population, whereas K14-ΔN–β-catenin, *Cby1* (this study), MMTV-Wnt1, and MMTV–β-catenin (Li et al., 2003) mice all contain an increased K6$^+$ population within the mammary epithelium. Second, we show that depletion of Pygo2 results in decreased expression of both artificial and physiological Wnt/β-catenin target genes, including BAT-gal, *Lef1*, c-Myc, and cyclin D1. Third, we demonstrate direct occupancy of Pygo2 at the known target loci. Finally and most importantly, we report a complete rescue of the Wnt/β-catenin–activated aberrant mammary outgrowth by the loss of epithelial Pygo2. Collectively, these results lend strong support to the notion that Pygo2 regulates the cellular and molecular events downstream of Wnt/β-catenin signaling; in its absence, ectopic Wnt/β-catenin signaling can no longer elicit its effect on mammary progenitor cells. As such, our work significantly extends the current understanding on the role of Wnt/β-catenin signaling in mammary stem/progenitor cell self-renewal.

Pygo2 and chromatin-activating histone methylation in mammary progenitor cells

While this work was in progress, Fiedler et al. (2008) reported in vitro evidence that several Pygo proteins, particularly human Pygo1, can directly bind H3K4me2 and H3K4me3. Our work now provides independent as well as in vivo evidence that Pygo2 directly binds to K4-methyl histone H3. That an H3K4me2/3 binding–deficient Pygo2 protein loses its ability to enhance colony formation strongly suggests that Pygo2 functions in mammary progenitor cell expansion by binding to H3K4me2/3. Moreover, we show that Pygo2 not only binds to but also facilitates the generation of additional H3K4me3 marks in both bulk chromatin and at specific Wnt target loci. This capacity to both "read" and "write" (Strahl and Allis, 2000; Fischle et al., 2003) H3 K4 methylation highlights the existence of a Pygo2-mediated positive feedback to achieve an active chromatin status.

The ability of Pygo2 to facilitate histone H3 trimethylation likely arises from its physical association with SET domain HMT complexes, as suggested by the observed Pygo2–WDR5 interaction in mammary progenitor cells. Interestingly, this interaction occurs in the absence of extracellular Wnt-like stimuli and independently of detectable Pygo2–β-catenin interaction. Consistently, we show that Pygo2 depletion results in decreased WDR5 occupancy and H3K4me3 not only at Wnt/β-catenin target loci but also in bulk chromatin in unstimulated mammary progenitor cells. Based on these results, we surmise that Pygo2 is bound to chromatin and facilitates H3 K4 trimethylation in the

anti-GST antibody. (F) Mapping residues in Pygo2 PHD required for H3K4me3 (b) or BCL9 HD1 (c) interaction. (a) Coomassie blue staining of GST, GST–Pygo2 PHD derivatives, and 6× His–BCL9 HD1 domain proteins purified from bacteria. GST pull-downs of histones were analyzed by Western blotting with anti-H3K4me3 (b), whereas nickel (6× His) pull-downs of GST-PHD derivatives were analyzed with anti-GST antibodies (c). (G) Synergistic interactions among H3K4me3–Pygo2–BCL9. Purified proteins were incubated as indicated and pulled down by nickel beads, and eluates were analyzed by Western blotting with the indicated antibodies. (H) Methyl histone H3 binding of Pygo2 is required for colony formation by MCF10A cells. (a) Representative images revealing the effects of exogenous Pygo2 derivatives are shown. (b) Quantification of three independent experiments. Error bars represent standard deviation. *, P = 1.0; **, P = 0.045; ‡, P = 0.010; and †, P = 0.030. P-values were calculated using two-tailed *t* tests assuming equal variance. Note that wild-type and mutant 2× Flag–flagged Pygo2 proteins were expressed at similar levels in infected cells (c). IB, immunoblot; IP, immunoprecipitation.
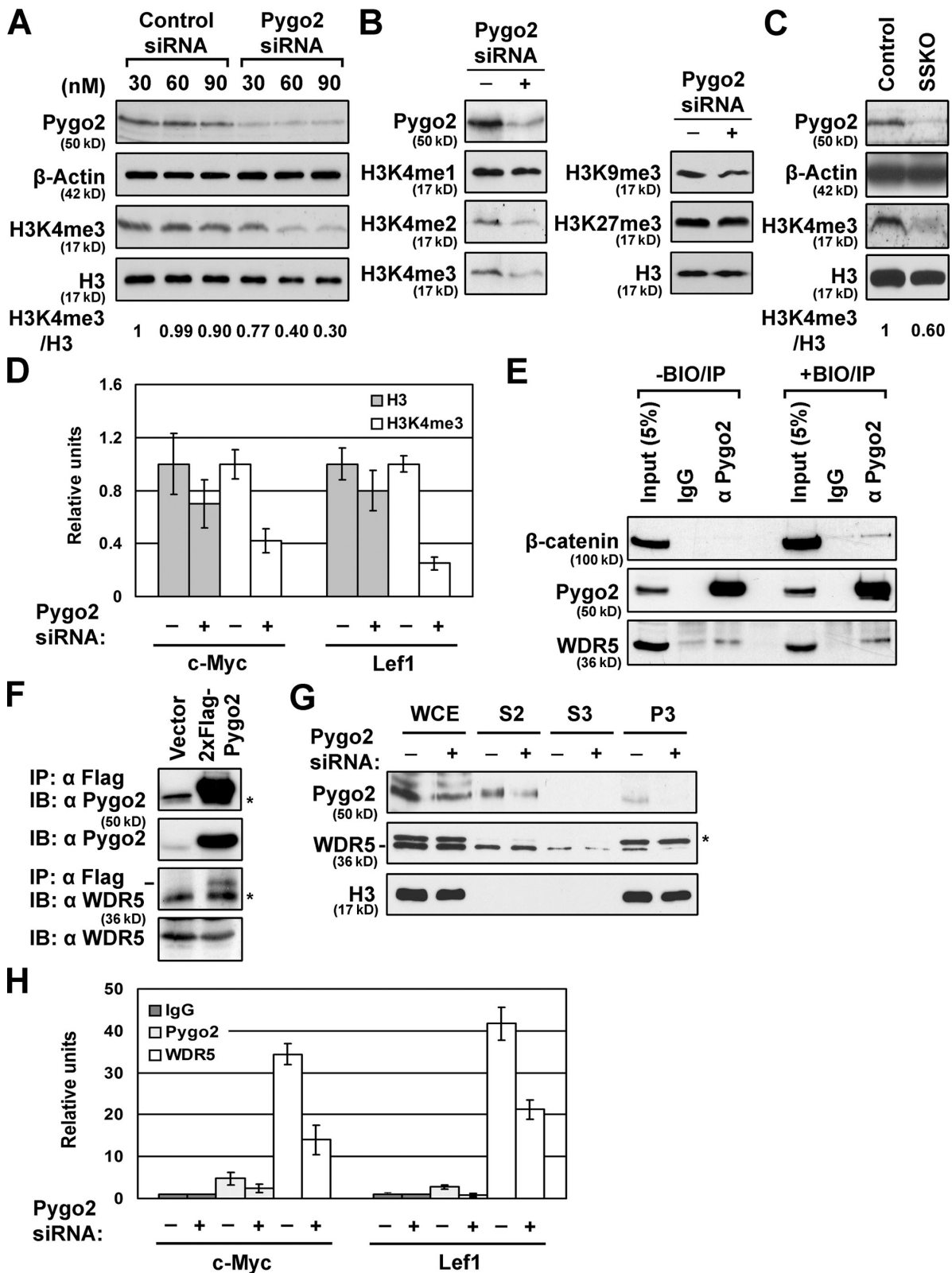
Figure 8. **Pygo2 regulates H3K4me3 levels by facilitating chromatin association of WDR5.** (A) Requirement of Pygo2 for global H3K4me3 in MCF10A cells. The H3K4me3/H3 ratio in cells treated with 30 nM of control siRNA was arbitrarily set to be 1. (B) Western blot analysis showing that Pygo2 knockdown specifically affects di- and trimethylation of H3 K4. (C) Reduced H3K4me3 levels in *Pygo2* SSKO mammary glands. The H3K4me3/H3 ratio in wild-type glands was arbitrarily set to be 1. (D) Results of ChIP experiments revealing reduced H3K4me3 at the c-Myc enhancer and *Lef1* promoter. Note that the total H3 levels at these loci are not significantly affected. (E) Association of Pygo2 with WDR5 in 293T cells with and without BIO treatment. (F) Pygo2–WDR5 interaction in MCF10A cells. Asterisks label cross-reacting IgGs. (G) Reduction of chromatin association of WDR5 upon knockdown of Pygo2 in MCF10A cells. The asterisk indicates a cross-reacting band. WCE, whole-cell extract; S2, soluble cytosolic fraction; S3, soluble nuclear fraction;

absence of Wnt signaling, providing a molecular basis for Wnt/β-catenin–independent biological functions of Pygo2 (Song et al., 2007; Nair et al., 2008). However, in Wnt-stimulated cells, simultaneous and synergistic interactions between Pygo2, H3K4me2/3, and BCL9/β-catenin at Wnt target promoters may significantly alter the free energy required for assembly of a macromolecular complex to bring about maximal transcriptional activation. In this way, Wnt signaling exploits Pygo2, a rather nonspecific chromatin effector to achieve maximal activation of specific target genes. That a global chromatin regulator regulates transcriptional output of a specific gene set is not unprecedented. For instance, although it has been well documented that WDR5 depletion dramatically affects global H3K4me3 levels (Wysocka et al., 2005), during osteoblast differentiation, WDR5 overexpression/depletion results in increased/decreased Wnt target gene expression, respectively (Zhu et al., 2008).

Although our data provide an underlying mechanism for a Wnt signaling coactivator function of Pygo proteins, we have not been able to obtain evidence supporting a role for Pygo2 in β-catenin nuclear localization in mammary progenitor cells. Few cells in developing mammary glands express nuclear β-catenin, making it difficult to convincingly demonstrate any possible reduction of such cells in Pygo2-deficient mice. We performed Western blot analysis on nuclear extracts isolated from MCF10A cells and those depleted for Pygo2 but failed to detect any significant decrease in the level of Wnt-stimulated nuclear β-catenin (unpublished data). Therefore, the function of Pygo2 in nuclear retention of β-catenin might be cell type dependent.

Chepko and Smith (1997) noted that the heterochromatin in mammary stem cells is lost in early progenitor cells but reappears in differentiated cells, demonstrating a correlation between open chromatin configuration and a mammary progenitor fate. Our findings now imply a causal link between Pygo2-facilitated chromatin activation and mammary progenitor cell expansion. Embryonic stem cells are also capable of expansive self-renewal, and their chromatin is indeed mostly open, as suggested by the abundance of H3K4me3 and acetylated histone H4 (also associated with active chromatin) and scarcity of K9 or K27 trimethylated histone H3 (Niwa, 2007). Therefore, a globally active chromatin conformation may be a key feature of expanding stem/progenitor cells, and the epigenetic function of Pygo2 in different stem/progenitor cell systems merits further investigation.

Relevance to breast cancer

The number of stem/progenitor cells in a given tissue is thought to be determined during critical developmental windows (Ginestier and Wicha, 2007). It follows that if breast cancer stem cells arise from normal mammary stem/progenitor cells, the number of cells that can serve as transformation targets may dictate cancer risk. In this context, Pygo2 may be a potential target of mammary tumorigenesis, particularly in cancers that are of a stem/progenitor cell origin. Consistent with this notion, Pygo2 expression is up-regulated in breast cancers and cancer cell lines (Andrews et al., 2007; unpublished data). Based on our loss of function data, it is reasonable to expect altered p21 expression in Pygo2-overexpressing cancer cells. Indeed, loss of p21 accelerates ras-induced mammary tumorigenesis (Adnane et al., 2000) and appears to be the underlying basis for hormonally responsive breast cancer cells to develop tamoxifen resistance (Abukhdeir et al., 2008). In the future, it will be worthwhile to directly explore the involvement of Pygo2 in stem/progenitor-derived breast cancers and cancer stem cells.

Currently, drugs that aim at correcting silencing epigenetic changes at select tumor suppressor loci are being tested in clinical trials for cancer therapy (Yoo and Jones, 2006). However, it had not been appreciated that such drugs may activate chromatin in an undesired manner that sets off uncontrollable normal as well as cancer stem cell expansion. The study of how normal activating epigenetic patterns are established and maintained in stem/progenitor cells and how alterations occur in cancer bears important implications on cancer therapy.

Materials and methods

Mice and antibodies

The generation and genotyping of null and floxed *Pygo2* alleles were performed as previously described (Li et al., 2007). *Pygo2*−/− embryos were obtained by *Pygo2*+/− heterozygote intercrosses. *Pygo2* SSKO mice were generated by crossing K14-Cre/*Pygo2*+/− males with *Pygo2*flox/flox or *Pygo2*flox/+ females. To confirm tissue-specific recombination, the epidermis was separated from the underlying dermis by overnight exposure of newborn back skin to dispase II (Roche) at 4°C as previously described (Kitano and Okada, 1983), and DNAs were prepared from isolated epidermis and dermis for genotyping. Sex was determined by PCR of a male-specific gene using the primers 5′-TTACATAATCACATGGAGAGCCA-3′ and 5′-GTCACATTTATGAGGATACGCC-3′. Estrus was determined by established morphological criteria. K14-ΔN–β-catenin and BAT-gal mice were gifts from E. Fuchs (The Rockefeller University, New York, NY) and S. Piccolo (University of Padova, Padova, Italy). All experiments have been approved by and conform to the regulatory guidelines of the International Animal Care and Use Committee of the University of California, Irvine.

α-Pygo2 rabbit polyclonal antibody was previously described (Li et al., 2007). Antibodies to K14 (chicken; 1:4,000), K6 (rabbit; 1:500), and GATA-3 were gifts from J. Segre (National Institutes of Health, Bethesda, MD). α-NKCC1 was a gift from J. Turner (National Institutes of Health, Bethesda, MD). Other antibodies were obtained commercially: α-ER (MC-20; Santa Cruz Biotechnology, Inc.); α-K18 (Developmental Studies Hybridoma Bank); α-H3, α-H3K4me1, α-H3K4me2, α-H3K4me3, α-H3K9me3, and α-H3K27me3 (Millipore); α-Flag and α–β-catenin (Sigma-Aldrich); α-WDR5 and α–β-actin (Abcam); and rabbit IgG and α-GST (Santa Cruz Biotechnology, Inc.).

Morphology, immunostaining, and whole-mount in situ hybridization

For whole-mount mammary gland staining, E18.5 skins were flattened on microscope slides, fixed overnight in Carnoy's solution (75% ethanol and 25% acetic acid), and stained with carmine alum as previously described (Sympson et al., 1994). Postnatal mammary glands were fixed in 60% ethanol, 30% CHCl₃, and 10% glacial acetic acid and similarly stained.

Indirect immunofluorescence was performed as previously described (Dai et al., 1998) using rabbit α-Pygo2 antiserum that was preadsorbed with tissue powder prepared from E15.5 *Pygo2*−/− embryos. FITC-conjugated goat anti–rabbit and rhodamine-conjugated goat anti–chicken or mouse secondary antibodies (Jackson ImmunoResearch Laboratories) were used, and slides were mounted in antifade medium (Vectashield H-1000; Vector Laboratories). Images were taken at room temperature with an inverted fluorescence microscope (Eclipse E600; Nikon) using Plan-Apochromat

P3, chromatin-enriched fraction. (H) ChIP analysis showing decreased WDR5 occupancy at the c-Myc enhancer and *Lef1* promoter in Pygo2-depleted MCF10A cells. (D and H) Error bars represent standard deviation. IB, immunoblot; IP, immunoprecipitation.

20× NA 0.75 or Plan-Fluor 40× NA 0.75 objectives (Nikon) and a camera (RT Slider; Diagnostic Instruments, Inc.) equipped with SPOT 4.0.9 software (Diagnostic Instruments, Inc.). Acquired images were processed by Photoshop CS 8.0 (Adobe).

Whole-mount in situ hybridizations were performed as previously described (Mackay et al., 2006) using a *Wnt10b* probe (Veltmaat et al., 2004) or a 710-bp fragment corresponding to nucleotides 1,034–1,743 of *Lef1* mRNA (GenBank/EMBL/DDBJ accession no. NM_010703). Images were acquired using an Eclipse E600 microscope.

Analysis of β-galactosidase expression
Analysis of BAT-gal expression was performed as previously described (Li et al., 2007). 10-μm transverse cryosections were counterstained with Nuclear Fast red. β-Galactosidase staining of adult mammary glands was performed as follows: 14-μm sections were fixed in 0.5% glutaraldehyde in 0.1 M phosphate buffer for 2 min, washed with 0.1 M phosphate buffer eight times, and transferred into freshly prepared X-gal staining solution containing 100 mM Na-phosphate buffer, pH 7.3, 1 mg/ml X-gal, 3 mM $K_3Fe(CN)_6$, 3 mM $K_4Fe(CN)_6$, and 1.3 mM $MgCl_2$. Incubation was performed at room temperature in the dark until signal appeared. The slides were subsequently counterstained with Nuclear Fast red and mounted with the Permount mounting medium (Thermo Fisher Scientific).

FACS analysis
Mammary glands from 10–12-wk-old virgin females were digested for 6 h at 37°C in RPMI 1640 containing 5% FBS, 300 U/ml collagenase, and 100 U/ml hyaluronidase. After vortexing and lysis of the red blood cells in NH_4Cl, a single-cell suspension was obtained by sequential dissociation of the fragments by gentle pipetting for 1–2 min in 0.25% trypsin and then for 2 min in 5 mg/ml dispase II plus 0.1 mg/ml DNase I (Sigma-Aldrich) followed by filtration through a 40-mm mesh. Staining was performed using the following antibodies and reagents: biotinylated CD31 (BD), biotinylated CD45 (BD), biotinylated TER119 (BD), streptavidin-allophycocyanin (BD), phycoerythrin Rat IgG2b, κ isotype control (BD), FITC Armenian Hamster IgG isotype control (BioLegend), CD24-phycoerythrin (BD), and CD29-FITC (BioLegend). Cell cycle analysis was performed as previously described (Gu and Chen, 2009). Cells were acquired on FACSCalibur (BD), and analysis was performed using FlowJo (Tree Star, Inc.).

Limiting dilution cell transplantation
Limiting dilution cell transplantation was performed essentially as previously described (Moraes et al., 2007). In brief, primary MECs isolated from two paired sets of control or *Pygo2* SSKO mice (three mice per genotype per set) were counted and resuspended in a 1:1 solution of PBS/Matrigel (BD). Cells of each genotype were injected at limiting dilutions (10,000, 5,000, 1,000, 500, and 250 cells per gland, in a total volume of 10 μl) into contralateral cleared fat pads of no. 4 mammary glands of 21-d-old female severe combined immunodeficiency Beige mice (Charles River Laboratories) using a 25-G needle attached to a 50-μl Hamilton glass syringe. 8–9 wk after transplantation, no. 4 glands were excised and stained as whole mounts. Glands showing at least 5% fat pad filling were scored as a positive take. Statistical analysis of the take rate was performed as previously described (Moraes et al., 2007). The data on fat pad filling were analyzed by a generalized linear model using the Gamma regression.

BrdU labeling and immunodetection
Pregnant mice were intraperitoneally injected with 50 μg/g body weight of BrdU in PBS. Embryos were taken 1 h after injection, cryosectioned at 10 μm, and fixed in 4% paraformaldehyde for 10 min followed by immunohistochemistry as previously described (Li et al., 2005). A weak hematoxylin counterstaining was performed, and cells within each mammary bud were counted to determine the percentage of BrdU-positive cells versus the total number of cells. Statistical significance was determined using Student's *t* test.

Cell culture, cloning, and mutagenesis
Primary MECs (2×10^4) isolated from 8–10-wk-old virgin females were plated on Matrigel (BD) per well in chamber slides (Laboratory-Tek II), cultured for 14 d, and fixed in 4% paraformaldehyde for 20 min at room temperature. Colonies were then permeabilized with PBS containing 0.5% Triton X-100 for 10 min at 4°C, followed by three 10–15-min rinses with PBS/glycine (130 mM NaCl, 7 mM Na_2HPO_4, and 3.5 mM NaH_2PO_4; 100 mM glycine) at room temperature. Nonspecific interactions were blocked by incubating with 200 μl/well of IF buffer (130 mM NaCl, 7 mM Na_2HPO_4, and 3.5 mM NaH_2PO_4; 7.7 mM NaN_3, 0.1% BSA, 0.2%

Triton X-100, and 0.05% Tween 20) containing 10% goat serum for 45–60 min at room temperature, after which indirect immunofluorescence was performed as described in Morphology, immunostaining, and whole-mount in situ hybridization.

MCF10A cells, human embryonic kidney 293T cells, and packaging 293GP2 cells were cultured as previously described (Furuta et al., 2006). The PHD of Pygo2 and HD1 domain of BCL9 were cloned by PCR from Pygo2 cDNA and cDNAs of human HaCaT cells, respectively. Point mutations were generated by site-directed mutagenesis (Agilent Technologies). DNA fragments were subcloned into pGEX4T-3 (GE Healthcare), pRSET-A (Invitrogen), pcDNA3.1–2× Flag, and pQCXIP (BD) for expression in bacteria or mammalian cells.

Protein purification and pull-down assays
GST- or 6× His–tagged fusion proteins were expressed in BL21(DE3)/pLysS strain and purified to near homogeneity as previously described (Shang et al., 2003). Fusion proteins were eluted with 10 mM glutathione or 200 mM imidazole where necessary. Purified calf thymus core histones (Worthington) were incubated with purified GST fusion proteins bound on beads for 3 h at 4°C. Up to 5 μg of histones and 10 μg of GST fusion proteins were used in each pull-down reaction. Beads were washed four times with binding buffer containing 50 mM Tris, pH 7.4, 300 mM NaCl, 0.5 mM EDTA, 0.5% NP-40, 1 mM PMSF, and protease inhibitors cocktail (Roche). Bound proteins were boiled with 2× sample buffer and analyzed by SDS-PAGE/Western blotting. For peptide pull-downs, 1 μg of biotinylated histone peptides (Millipore) were incubated with 1 μg of GST fusion proteins in binding buffer (50 mM Tris, pH 7.4, 150 mM NaCl, 0.1% NP-40, 1 mM PMSF, and protease inhibitor cocktail) overnight at 4°C. After 1 h of incubation, streptavidin beads (Thermo Fisher Scientific) were washed three times and subjected to Western blot analysis. For binding assays between BCL9-HD1 and GST fusion proteins, 6× His–HD1 were incubated with an equal amount of GST–Pygo2 PHD derivatives in binding buffer containing 10 mM imidazole, and protein complexes were captured by nickel–nitrilotriacetic acid beads (QIAGEN).

Coimmunoprecipitation and Western blotting
Cells were either untreated or treated with 2 μM BIO (Sigma-Aldrich) for 2 h in culture media, and nuclear extracts were prepared with treatment of benzonase (EMD) as previously described (McKinnell et al., 2008). Primary antibody of α-Pygo2 or control normal rabbit IgG was incubated at 2 μg per 500 μg of nuclear extract overnight at 4°C before being collected with protein A/G beads. Immunocomplexes were washed four times with nuclear lysis buffer and eluted by boiling in 2× sample buffer. Samples were resolved by 12% SDS-PAGE and immunoblotted with the indicated antibodies.

Retroviral infection and colony formation assay
Recombinant retrovirus expressing 2× Flag–Pygo2 derivatives were generated as previously described (Wang et al., 2007). In brief, packaging cells 293GP2 were cotransfected with pVSV-G and a retroviral vector pQCXIP expressing 2× Flag–Pygo2 derivatives. Titered viruses were then used to infect MCF10A cells for 48 h before selection with 2.5 μg/ml puromycin for an additional 48 h. The pool of infected cells was then counted and plated at 1,000 cells per 60-mm dish in triplicate in the presence of 0.4 μg/ml puromycin. After 2 wk, colonies were fixed, stained with methyl blue, and counted as previously described (Chen et al., 1999).

ChIP and chromatin fractionation
MCF10A cell were transfected with Pygo2 siRNA or negative control siRNA (Applied Biosystems) using Lipofectamine 2000 (Invitrogen) according to manufacture's instructions. Cells were harvested 72 h after transfection and were either lysed in sample buffer for Western blot analysis or fixed in 1% formaldehyde for subsequent ChIP analysis according to the protocol from Millipore. Real-time PCR quantification of ChIP signals was performed in triplicate using SYBR Green Supermix (Bio-Rad Laboratories) and primers for c-Myc enhancer (Sierra et al., 2006) or *Lef1* promoter (forward, 5′-TCCTGGATTCCTTCACCAAC-3′; reverse, 5′-TCAGGCTGCTGA-ACATTGAA-3′). ChIP signals were quantified relative to normal IgG or control histone H3 signals where indicated.

Biochemical chromatin fractionation was performed as previously described (Mendez and Stillman, 2000). MCF10A cells were transfected with Pygo2 or control siRNA for 72 h and harvested for preparation of either whole cell extract or fractions enriched for cytoplasmic, nuclear soluble, or chromatin. Protein samples were analyzed by Western blotting with specific antibodies as indicated.

Online supplemental material

Fig. S1 shows alveolar and functional defects of Pygo2-deficient mammary glands. Fig. S2 shows normal differentiation and biochemistry in *Pygo2* SSKO mammary epithelium. Fig. S3 shows MCF10A as an alternative cell culture model to study mammary progenitor cells. Fig. S4 shows whole-mount in situ hybridization demonstrating normal *Wnt10b* expression in Pygo2-deficient mammary epithelium. Online supplemental material is available at http://www.jcb.org/cgi/content/full/jcb.200810133/DC1.

References

Abukhdeir, A.M., M.I. Vitolo, P. Argani, A.M. De Marzo, B. Karakas, H. Konishi, J.P. Gustin, J. Lauring, J.P. Garay, C. Pendleton, et al. 2008. Tamoxifen-stimulated growth of breast cancer due to p21 loss. *Proc. Natl. Acad. Sci. USA*. 105:288–293.

Adnane, J., R.J. Jackson, S.V. Nicosia, A.B. Cantor, W.J. Pledger, and S.M. Sebti. 2000. Loss of p21WAF1/CIP1 accelerates Ras oncogenesis in a transgenic/knockout mammary cancer model. *Oncogene*. 19:5338–5347.

Andl, T., K. Ahn, A. Kairo, E.Y. Chu, L. Wine-Lee, S.T. Reddy, N.J. Croft, J.A. Cebra-Thomas, D. Metzger, P. Chambon, et al. 2004. Epithelial Bmpr1a regulates differentiation and proliferation in postnatal hair follicles and is essential for tooth development. *Development*. 131:2257–2268.

Andrews, P.G., B.B. Lake, C. Popadiuk, and K.R. Kao. 2007. Requirement of Pygopus 2 in breast cancer. *Int. J. Oncol.* 30:357–363.

Asselin-Labat, M.L., K.D. Sutherland, H. Barker, R. Thomas, M. Shackleton, N.C. Forrest, L. Hartley, L. Robb, F.G. Grosveld, J. van der Wees, et al. 2007. Gata-3 is an essential regulator of mammary-gland morphogenesis and luminal-cell differentiation. *Nat. Cell Biol.* 9:201–209.

Ball, S.M. 1998. The development of the terminal end bud in the prepubertal-pubertal mouse mammary gland. *Anat. Rec.* 250:459–464.

Barker, N., G. Huls, V. Korinek, and H. Clevers. 1999. Restricted high level expression of Tcf-4 protein in intestinal and mammary gland epithelium. *Am. J. Pathol.* 154:29–35.

Belenkaya, T.Y., C. Han, H.J. Standley, X. Lin, D.W. Houston, and J. Heasman. 2002. pygopus Encodes a nuclear protein essential for wingless/Wnt signaling. *Development*. 129:4089–4101.

Bienz, M. 2006. The PHD finger, a nuclear protein-interaction domain. *Trends Biochem. Sci.* 31:35–40.

Boras-Granic, K., H. Chang, R. Grosschedl, and P.A. Hamel. 2006. Lef1 is required for the transition of Wnt signaling from mesenchymal to epithelial cells in the mouse embryonic mammary gland. *Dev. Biol.* 295:219–231.

Chen, C.F., P.L. Chen, Q. Zhong, Z.D. Sharp, and W.H. Lee. 1999. Expression of BRC repeats in breast cancer cells disrupts the BRCA2-Rad51 complex and leads to radiation hypersensitivity and loss of G(2)/M checkpoint control. *J. Biol. Chem.* 274:32931–32935.

Cheng, T., N. Rodrigues, H. Shen, Y. Yang, D. Dombkowski, M. Sykes, and D.T. Scadden. 2000. Hematopoietic stem cell quiescence maintained by p21cip1/waf1. *Science*. 287:1804–1808.

Chepko, G., and G.H. Smith. 1997. Three division-competent, structurally-distinct cell populations contribute to murine mammary epithelial renewal. *Tissue Cell*. 29:239–253.

Clarke, R.B. 2005. Isolation and characterization of human mammary stem cells. *Cell Prolif.* 38:375–386.

Clarke, R.B., K. Spence, E. Anderson, A. Howell, H. Okano, and C.S. Potten. 2005. A putative human breast stem cell population is enriched for steroid receptor-positive cells. *Dev. Biol.* 277:443–456.

Cui, K., C. Zang, T.Y. Roh, D.E. Schones, R.W. Childs, W. Peng, and K. Zhao. 2009. Chromatin signatures in multipotent human hematopoietic stem cells indicate the fate of bivalent genes during differentiation. *Cell Stem Cell*. 4:80–93.

Dai, X., C. Schonbaum, L. Degenstein, W. Bai, A. Mahowald, and E. Fuchs. 1998. The ovo gene required for cuticle formation and oogenesis in flies is involved in hair formation and spermatogenesis in mice. *Genes Dev.* 12:3452–3463.

Dou, Y., T.A. Milne, A.J. Ruthenburg, S. Lee, J.W. Lee, G.L. Verdine, C.D. Allis, and R.G. Roeder. 2006. Regulation of MLL1 H3K4 methyltransferase activity by its core components. *Nat. Struct. Mol. Biol.* 13:713–719.

Fiedler, M., M.J. Sanchez-Barrena, M. Nekrasov, J. Mieszczanek, V. Rybin, J. Muller, P. Evans, and M. Bienz. 2008. Decoding of methylated histone H3 tail by the Pygo-BCL9 Wnt signaling complex. *Mol. Cell*. 30:507–518.

Filali, M., N. Cheng, D. Abbott, V. Leontiev, and J.F. Engelhardt. 2002. Wnt-3A/beta-catenin signaling induces transcription from the LEF-1 promoter. *J. Biol. Chem.* 277:33398–33410.

Fischle, W., Y. Wang, and C.D. Allis. 2003. Histone and chromatin cross-talk. *Curr. Opin. Cell Biol.* 15:172–183.

Furuta, S., J.M. Wang, S. Wei, Y.M. Jeng, X. Jiang, B. Gu, P.L. Chen, E.Y. Lee, and W.H. Lee. 2006. Removal of BRCA1/CtIP/ZBRK1 repressor complex on ANG1 promoter leads to accelerated mammary tumor growth contributed by prominent vasculature. *Cancer Cell*. 10:13–24.

Gat, U., R. DasGupta, L. Degenstein, and E. Fuchs. 1998. De Novo hair follicle morphogenesis and hair tumors in mice expressing a truncated beta-catenin in skin. *Cell*. 95:605–614.

Ginestier, C., and M.S. Wicha. 2007. Mammary stem cell number as a determinate of breast cancer risk. *Breast Cancer Res.* 9:109.

Grimm, S.L., W. Bu, M.A. Longley, D.R. Roop, Y. Li, and J.M. Rosen. 2006. Keratin 6 is not essential for mammary gland development. *Breast Cancer Res.* 8:R29.

Gu, B., and P.L. Chen. 2009. Expression of PCNA-binding domain of CtIP, a motif required for CtIP localization at DNA replication foci, causes DNA damage and activation of DNA damage checkpoint. *Cell Cycle*. 8:1409–1420.

He, T.C., A.B. Sparks, C. Rago, H. Hermeking, L. Zawel, L.T. da Costa, P.J. Morin, B. Vogelstein, and K.W. Kinzler. 1998. Identification of c-MYC as a target of the APC pathway. *Science*. 281:1509–1512.

Hennighausen, L., and G.W. Robinson. 2001. Signaling pathways in mammary gland development. *Dev. Cell*. 1:467–475.

Hovanes, K., T.W. Li, J.E. Munguia, T. Truong, T. Milovanovic, J. Lawrence Marsh, R.F. Holcombe, and M.L. Waterman. 2001. Beta-catenin-sensitive isoforms of lymphoid enhancer factor-1 are selectively expressed in colon cancer. *Nat. Genet.* 28:53–57.

Jessen, S., B. Gu, and X. Dai. 2008. Pygopus and the Wnt signaling pathway: a diverse set of connections. *Bioessays*. 30:448–456.

Kenney, N.J., G.H. Smith, E. Lawrence, J.C. Barrett, and D.S. Salomon. 2001. Identification of stem cell units in the terminal end bud and duct of the mouse mammary gland. *J. Biomed. Biotechnol.* 1:133–143.

Kippin, T.E., D.J. Martens, and D. van der Kooy. 2005. p21 loss compromises the relative quiescence of forebrain stem cell proliferation leading to exhaustion of their proliferation capacity. *Genes Dev.* 19:756–767.

Kitano, Y., and N. Okada. 1983. Separation of the epidermal sheet by dispase. *Br. J. Dermatol.* 108:555–560.

Kouros-Mehr, H., E.M. Slorach, M.D. Sternlicht, and Z. Werb. 2006. GATA-3 maintains the differentiation of the luminal cell fate in the mammary gland. *Cell*. 127:1041–1055.

Kramps, T., O. Peter, E. Brunner, D. Nellen, B. Froesch, S. Chatterjee, M. Murone, S. Zullig, and K. Basler. 2002. Wnt/wingless signaling requires BCL9/legless-mediated recruitment of pygopus to the nuclear beta-catenin-TCF complex. *Cell*. 109:47–60.

Li, B., M. Nair, D.R. Mackay, V. Bilanchone, M. Hu, M. Fallahi, H. Song, Q. Dai, P.E. Cohen, and X. Dai. 2005. Ovol1 regulates meiotic pachytene progression during spermatogenesis by repressing Id2 expression. *Development*. 132:1463–1473.

Li, B., C. Rheaume, A. Teng, V. Bilanchone, J.E. Munguia, M. Hu, S. Jessen, S. Piccolo, M.L. Waterman, and X. Dai. 2007. Developmental phenotypes and reduced Wnt signaling in mice deficient for pygopus 2. *Genesis*. 45:318–325.

Li, Y., B. Welm, K. Podsypanina, S. Huang, M. Chamorro, X. Zhang, T. Rowlands, M. Egeblad, P. Cowin, Z. Werb, et al. 2003. Evidence that transgenes encoding components of the Wnt signaling pathway preferentially induce mammary cancers from progenitor cells. *Proc. Natl. Acad. Sci. USA*. 100:15853–15858.

Lindvall, C., N.C. Evans, C.R. Zylstra, Y. Li, C.M. Alexander, and B.O. Williams. 2006. The Wnt signaling receptor Lrp5 is required for mammary ductal stem cell activity and Wnt1-induced tumorigenesis. *J. Biol. Chem.* 281:35081–35087.

Mackay, D.R., M. Hu, B. Li, C. Rheaume, and X. Dai. 2006. The mouse Ovol2 gene is required for cranial neural tube development. *Dev. Biol.* 291:38–52.

Mailleux, A.A., B. Spencer-Dene, C. Dillon, D. Ndiaye, C. Savona-Baron, N. Itoh, S. Kato, C. Dickson, J.P. Thiery, and S. Bellusci. 2002. Role of FGF10/ FGFR2b signaling during mammary gland development in the mouse embryo. *Development.* 129:53–60.

Maretto, S., M. Cordenonsi, S. Dupont, P. Braghetta, V. Broccoli, A.B. Hassan, D. Volpin, G.M. Bressan, and S. Piccolo. 2003. Mapping Wnt/beta-catenin signaling during mouse development and in colorectal tumors. *Proc. Natl. Acad. Sci. USA.* 100:3299–3304.

McKinnell, I.W., J. Ishibashi, F. Le Grand, V.G. Punch, G.C. Addicks, J.F. Greenblatt, F.J. Dilworth, and M.A. Rudnicki. 2008. Pax7 activates myogenic genes by recruitment of a histone methyltransferase complex. *Nat. Cell Biol.* 10:77–84.

Mendez, J., and B. Stillman. 2000. Chromatin association of human origin recognition complex, cdc6, and minichromosome maintenance proteins during the cell cycle: assembly of prereplication complexes in late mitosis. *Mol. Cell. Biol.* 20:8602–8612.

Miyoshi, K., J.M. Shillingford, G.H. Smith, S.L. Grimm, K.U. Wagner, T. Oka, J.M. Rosen, G.W. Robinson, and L. Hennighausen. 2001. Signal transducer and activator of transcription (Stat) 5 controls the proliferation and differentiation of mammary alveolar epithelium. *J. Cell Biol.* 155:531–542.

Moore-Hoon, M.L., and R.J. Turner. 1998. Molecular and topological characterization of the rat parotid Na+-K+-2Cl- cotransporter1. *Biochim. Biophys. Acta.* 1373:261–269.

Moraes, R.C., X. Zhang, N. Harrington, J.Y. Fung, M.F. Wu, S.G. Hilsenbeck, D.C. Allred, and M.T. Lewis. 2007. Constitutive activation of smoothened (SMO) in mammary glands of transgenic mice leads to increased proliferation, altered differentiation and ductal dysplasia. *Development.* 134:1231–1242.

Nair, M., I. Nagamori, P. Sun, D.P. Mishra, C. Rheaume, B. Li, P. Sassone-Corsi, and X. Dai. 2008. Nuclear regulator Pygo2 controls spermiogenesis and histone H3 acetylation. *Dev. Biol.* 320:446–455.

Neve, R.M., K. Chin, J. Fridlyand, J. Yeh, F.L. Baehner, T. Fevr, L. Clark, N. Bayani, J.P. Coppe, F. Tong, et al. 2006. A collection of breast cancer cell lines for the study of functionally distinct cancer subtypes. *Cancer Cell.* 10:515–527.

Niwa, H. 2007. Open conformation chromatin and pluripotency. *Genes Dev.* 21:2671–2676.

Parker, D.S., J. Jemison, and K.M. Cadigan. 2002. Pygopus, a nuclear PHD-finger protein required for Wingless signaling in *Drosophila. Development.* 129:2565–2576.

Pena, P.V., F. Davrazou, X. Shi, K.L. Walter, V.V. Verkhusha, O. Gozani, R. Zhao, and T.G. Kutateladze. 2006. Molecular mechanism of histone H3K4me3 recognition by plant homeodomain of ING2. *Nature.* 442:100–103.

Pietersen, A.M., B. Evers, A.A. Prasad, E. Tanger, P. Cornelissen-Steijger, J. Jonkers, and M. van Lohuizen. 2008. Bmi1 regulates stem cells and proliferation and differentiation of committed cells in mammary epithelium. *Curr. Biol.* 18:1094–1099.

Sato, N., L. Meijer, L. Skaltsounis, P. Greengard, and A.H. Brivanlou. 2004. Maintenance of pluripotency in human and mouse embryonic stem cells through activation of Wnt signaling by a pharmacological GSK-3-specific inhibitor. *Nat. Med.* 10:55–63.

Schwab, K.R., L.T. Patterson, H.A. Hartman, N. Song, R.A. Lang, X. Lin, and S.S. Potter. 2007. Pygo1 and Pygo2 roles in Wnt signaling in mammalian kidney development. *BMC Biol.* 5:15.

Shackleton, M., F. Vaillant, K.J. Simpson, J. Stingl, G.K. Smyth, M.L. Asselin-Labat, L. Wu, G.J. Lindeman, and J.E. Visvader. 2006. Generation of a functional mammary gland from a single stem cell. *Nature.* 439:84–88.

Shang, Y.L., A.J. Bodero, and P.L. Chen. 2003. NFBD1, a novel nuclear protein with signature motifs of FHA and BRCT, and an internal 41-amino acid repeat sequence, is an early participant in DNA damage response. *J. Biol. Chem.* 278:6323–6329.

Shi, X., T. Hong, K.L. Walter, M. Ewalt, E. Michishita, T. Hung, D. Carney, P. Pena, F. Lan, M.R. Kaadige, et al. 2006. ING2 PHD domain links histone H3 lysine 4 methylation to active gene repression. *Nature.* 442:96–99.

Sierra, J., T. Yoshida, C.A. Joazeiro, and K.A. Jones. 2006. The APC tumor suppressor counteracts beta-catenin activation and H3K4 methylation at Wnt target genes. *Genes Dev.* 20:586–600.

Sims, R.J. III, K. Nishioka, and D. Reinberg. 2003. Histone lysine methylation: a signature for chromatin function. *Trends Genet.* 19:629–639.

Sleeman, K.E., H. Kendrick, D. Robertson, C.M. Isacke, A. Ashworth, and M.J. Smalley. 2007. Dissociation of estrogen receptor expression and in vivo stem cell activity in the mammary gland. *J. Cell Biol.* 176:19–26.

Smith, G.H. 2005. Stem cells and mammary cancer in mice. *Stem Cell Rev.* 1:215–223.

Smith, G.H., T. Mehrel, and D.R. Roop. 1990. Differential keratin gene expression in developing, differentiating, preneoplastic, and neoplastic mouse mammary epithelium. *Cell Growth Differ.* 1:161–170.

Song, N., K.R. Schwab, L.T. Patterson, T. Yamaguchi, X. Lin, S.S. Potter, and R.A. Lang. 2007. pygopus 2 has a crucial, Wnt pathway-independent function in lens induction. *Development.* 134:1873–1885.

Stingl, J., P. Eirew, I. Ricketson, M. Shackleton, F. Vaillant, D. Choi, H.I. Li, and C.J. Eaves. 2006. Purification and unique properties of mammary epithelial stem cells. *Nature.* 439:993–997.

Strahl, B.D., and C.D. Allis. 2000. The language of covalent histone modifications. *Nature.* 403:41–45.

Sympson, C.J., R.S. Talhouk, C.M. Alexander, J.R. Chin, S.M. Clift, M.J. Bissell, and Z. Werb. 1994. Targeted expression of stromelysin-1 in mammary gland provides evidence for a role of proteinases in branching morphogenesis and the requirement for an intact basement membrane for tissue-specific gene expression. *J. Cell Biol.* 125:681–693.

Takemaru, K., S. Yamaguchi, Y.S. Lee, Y. Zhang, R.W. Carthew, and R.T. Moon. 2003. Chibby, a nuclear beta-catenin-associated antagonist of the Wnt/ Wingless pathway. *Nature.* 422:905–909.

Taverna, S.D., S. Ilin, R.S. Rogers, J.C. Tanny, H. Lavender, H. Li, L. Baker, J. Boyle, L.P. Blair, B.T. Chait, et al. 2006. Yng1 PHD finger binding to H3 trimethylated at K4 promotes NuA3 HAT activity at K14 of H3 and transcription at a subset of targeted ORFs. *Mol. Cell.* 24:785–796.

Tetsu, O., and F. McCormick. 1999. Beta-catenin regulates expression of cyclin D1 in colon carcinoma cells. *Nature.* 398:422–426.

Thompson, B., F. Townsley, R. Rosin-Arbesfeld, H. Musisi, and M. Bienz. 2002. A new nuclear component of the Wnt signalling pathway. *Nat. Cell Biol.* 4:367–373.

Topley, G.I., R. Okuyama, J.G. Gonzales, C. Conti, and G.P. Dotto. 1999. p21(WAF1/Cip1) functions as a suppressor of malignant skin tumor formation and a determinant of keratinocyte stem-cell potential. *Proc. Natl. Acad. Sci. USA.* 96:9089–9094.

Townsley, F.M., B. Thompson, and M. Bienz. 2004. Pygopus residues required for its binding to Legless are critical for transcription and development. *J. Biol. Chem.* 279:5177–5183.

van de Wetering, M., E. Sancho, C. Verweij, W. de Lau, I. Oving, A. Hurlstone, K. van der Horn, E. Batlle, D. Coudreuse, A.P. Haramis, et al. 2002. The beta-catenin/TCF-4 complex imposes a crypt progenitor phenotype on colorectal cancer cells. *Cell.* 111:241–250.

van Genderen, C., R.M. Okamura, I. Farinas, R.G. Quo, T.G. Parslow, L. Bruhn, and R. Grosschedl. 1994. Development of several organs that require inductive epithelial- mesenchymal interactions is impaired in LEF-1-deficient mice. *Genes Dev.* 8:2691–2703.

Veltmaat, J.M., A.A. Mailleux, J.P. Thiery, and S. Bellusci. 2003. Mouse embryonic mammogenesis as a model for the molecular regulation of pattern formation. *Differentiation.* 71:1–17.

Veltmaat, J.M., W. Van Veelen, J.P. Thiery, and S. Bellusci. 2004. Identification of the mammary line in mouse by Wnt10b expression. *Dev. Dyn.* 229:349–356.

Veltmaat, J.M., F. Relaix, L.T. Le, K. Kratochwil, F.G. Sala, W. van Veelen, R. Rice, B. Spencer-Dene, A.A. Mailleux, D.P. Rice, et al. 2006. Gli3-mediated somitic Fgf10 expression gradients are required for the induction and patterning of mammary epithelium along the embryonic axes. *Development.* 133:2325–2335.

Voronina, V.A., K. Takemaru, P. Treuting, D. Love, B.R. Grubb, A.M. Hajjar, A. Adams, F.Q. Li, and R.T. Moon. 2009. Inactivation of Chibby affects function of motile airway cilia. *J. Cell Biol.* 185:225–233.

Wang, X., C.F. Chen, P.R. Baker, P.L. Chen, P. Kaiser, and L. Huang. 2007. Mass spectrometric characterization of the affinity-purified human 26S proteasome complex. *Biochemistry.* 46:3553–3565.

Woodward, W.A., M.S. Chen, F. Behbod, and J.M. Rosen. 2005. On mammary stem cells. *J. Cell Sci.* 118:3585–3594.

Wysocka, J., T. Swigut, T.A. Milne, Y. Dou, X. Zhang, A.L. Burlingame, R.G. Roeder, A.H. Brivanlou, and C.D. Allis. 2005. WDR5 associates with histone H3 methylated at K4 and is essential for H3 K4 methylation and vertebrate development. *Cell.* 121:859–872.

Wysocka, J., T. Swigut, H. Xiao, T.A. Milne, S.Y. Kwon, J. Landry, M. Kauer, A.J. Tackett, B.T. Chait, P. Badenhorst, et al. 2006. A PHD finger of NURF couples histone H3 lysine 4 trimethylation with chromatin remodelling. *Nature.* 442:86–90.

Yoo, C.B., and P.A. Jones. 2006. Epigenetic therapy of cancer: past, present and future. *Nat. Rev. Drug Discov.* 5:37–50.

Zambrowicz, B.P., A. Imamoto, S. Fiering, L.A. Herzenberg, W.G. Kerr, and P. Soriano. 1997. Disruption of overlapping transcripts in the ROSA beta geo 26 gene trap strain leads to widespread expression of beta-galactosidase in mouse embryos and hematopoietic cells. *Proc. Natl. Acad. Sci. USA.* 94:3789–3794.

Zhu, E.D., M.B. Demay, and F. Gori. 2008. Wdr5 is essential for osteoblast differentiation. *J. Biol. Chem.* 283:7361–7367.